



**HAL**  
open science

## The 4GFOR model – Coupling 4G early diagenesis and benthic foraminiferal ecology

Frans Jorissen, Stephen Meyers, Boris Kelly-Gerreyn, Louison Huchet, Aurélia Mouret, Pierre Anschutz

► **To cite this version:**

Frans Jorissen, Stephen Meyers, Boris Kelly-Gerreyn, Louison Huchet, Aurélia Mouret, et al.. The 4GFOR model – Coupling 4G early diagenesis and benthic foraminiferal ecology. *Marine Micropaleontology*, 2022, 170, pp.102078. 10.1016/j.marmicro.2021.102078 . hal-03925911

**HAL Id: hal-03925911**

**<https://hal.science/hal-03925911>**

Submitted on 8 Dec 2023

**HAL** is a multi-disciplinary open access archive for the deposit and dissemination of scientific research documents, whether they are published or not. The documents may come from teaching and research institutions in France or abroad, or from public or private research centers.

L'archive ouverte pluridisciplinaire **HAL**, est destinée au dépôt et à la diffusion de documents scientifiques de niveau recherche, publiés ou non, émanant des établissements d'enseignement et de recherche français ou étrangers, des laboratoires publics ou privés.

# The 4GFOR Model – coupling 4G Early Diagenesis and Benthic Foraminiferal Ecology

Frans J. Jorissen<sup>1\*</sup>, Stephen R. Meyers<sup>2</sup>, Boris A. Kelly-Gerreyn<sup>3</sup>, Louison Huchet<sup>1</sup>, Aurélia Mouret<sup>1</sup> and Pierre Anschutz<sup>4</sup>

<sup>1</sup>UMR CNRS 6112 LPG-BIAF, Angers University, France

<sup>2</sup>University of Wisconsin, Department of Geoscience, Madison, USA

<sup>3</sup>Mount Waverley, Melbourne, Victoria 3149, Australia

<sup>4</sup>Univ. Bordeaux, CNRS, EPOC, EPHE, UMR 5805, F-33600 Pessac, France

\*Corresponding author: Frans J. Jorissen, UMR CNRS 6112 LPG-BIAF, Université d'Angers, 2, Boulevard Lavoisier, 49045 Angers Cedex, France. Email address : [frans.jorissen@univ-angers.fr](mailto:frans.jorissen@univ-angers.fr)

## Author Contributions

FJJ: conceptualisation, data management, model testing, writing. SRM: model development, writing. BAKG: model development, writing. LH: model testing, writing. AM: early diagenesis modeling, writing. PA: early diagenesis modeling, data management, writing.

## Abstract

The 4GFOR model presented in this paper combines the OMEXDIA model of Soetaert et al. (1996) with four theoretical species of benthic foraminifera. The geochemical part of the model simulates the succession of early diagenetic redox reactions in the superficial sediment layers. The four theoretical foraminiferal species, which each represent a group of biological species with comparable microhabitats, differ by their limitations with respect to oxygen and nitrate concentration and their ability to feed on different organic matter types. The foraminiferal model is a transformation model in which different proportions of four types of organic matter with different reactivity are attributed to each of the theoretical species. The model has been manually tuned and tested on a large data set from two stations, at 1000 and 550 m depth, in the Bay of Biscay. The model adequately simulates the vertical distribution of shallow, intermediate and deep infaunal species. The 4GFOR model can be used to test several hypotheses concerning foraminiferal ecology. The model has already allowed us to conclude that it is high unlikely that shallow infaunal taxa feed exclusively on the most labile part of the organic matter flux, since it was unable to reproduce the field observations while using this hypothesis. Another important conclusion based on our preliminary model results is that the absence of deep infaunal taxa close to the sediment surface may be explained by their decreasing competitiveness in well oxygenated environments. In the future, the inversion of the 4GFOR model may yield a powerful paleoceanographic tool, enabling us to reconstruct major limiting environmental factors (oxygen and nitrate concentrations; quantity and quality of the organic flux to the ocean floor) from benthic foraminiferal assemblage data.

## Keywords

Benthic foraminifera, ecology, microhabitats, early diagenesis, model.

## 43 1. Introduction

44 Since the pioneering work of Corliss and his colleagues in the 1980's (Corliss, 1985; Corliss & Chen  
45 1988; Corliss and Emerson, 1990) – which has been fully confirmed by a number of subsequent  
46 studies (i.e., Gooday, 1986; Mackensen and Douglas, 1989; McCorkle et al. 1990; Rathburn & Corliss,  
47 1994; Jorissen et al., 1998) – we know that in open marine settings, there is a vertical succession of  
48 benthic foraminiferal species in the surface sediment. This species succession, which appears to be  
49 closely related with the well-known succession of redox layers in the surface sediment (e.g., Froelich  
50 et al., 1979, Canfield et al., 1993) may be expanded over several centimetres (up to ~10 cm at most)  
51 or be compressed in the first few millimetres of the sediment. Despite of this vertical variability, the  
52 succession of foraminiferal species is always the same (Jorissen, 1999a). Consequently, foraminiferal  
53 species may be considered as shallow, intermediate or deep infaunal, not so much on the basis of the  
54 exact depth at which they are found in the sediment column, which can vary considerably, but rather  
55 on their relative position in the vertical species succession (Jorissen et al., 2007).

56 Following earlier suggestions of Shirayama (1984), Corliss and Emerson (1990) and Loubere et al.  
57 (1993), Jorissen et al. (1995) proposed the so-called TROX-model, which hypothesized that the  
58 vertical penetration depth of foraminiferal species into the sediment is determined by food  
59 availability in oligotrophic ecosystems, but would be limited by redox conditions (especially by pore  
60 water oxygen concentration and by the presence of toxic dissolved sulphides) in eutrophic settings.  
61 Different requirements with respect to these limiting factors would then explain the specific  
62 microhabitats of individual species. Indirectly, the TROX model also explains biodiversity trends,  
63 which are strongly affected by the availability or not of ecological niches deeper in the sediment. This  
64 conceptual model has since been confirmed by a large number of observational studies, and it has  
65 also been proposed to explain macrofaunal distribution patterns (Carney, 2005).

66 Since 1995, several authors have tried to further elaborate upon the TROX model, by integrating  
67 bioturbation (Van der Zwaan et al., 1999), or by coupling the foraminiferal distribution with several  
68 redox species (Koho et al., 2015), and not only with oxygen, as in the original model. In the 25 years  
69 since the publication of the TROX model, we have also learned a lot about benthic foraminiferal  
70 ecology. After the ground-breaking publications of Risgaard-Petersen et al. (2006), Høglund et al.  
71 (2008), Pina-Ochoa et al. (2010) and Bernhard et al. (2012), we know that many species are capable  
72 of storing nitrate in their protoplasm, and at least some of these species are capable of respiring  
73 nitrate when confronted with anoxia. For other taxa, a capability to sequester chloroplasts from  
74 consumed diatoms has been shown (e.g., Lee and Anderson, 1991; Bernhard and Bowser, 1999). The  
75 foraminifera are able to keep these intracellular chloroplasts active for several weeks, showing  
76 another foraminiferal strategy for survival under strongly adverse conditions (Jauffrais et al., 2016).  
77 And finally, a last group of species may survive adverse conditions by entering into a state of  
78 dormancy, with a strongly diminished metabolic rate (Bernhard and Alve, 1997; Ross and Hallock,  
79 2016).

80 The presence of an alternative metabolic pathway, in facultatively anaerobic taxa, as well as the  
81 other metabolic adaptations, explains why most benthic foraminiferal species are tolerant to strong  
82 hypoxia (at least down to ~0.5 ml/l, or 22  $\mu\text{mol/l}$ ; Jorissen et al., 2007). This also explains how  
83 foraminifera can survive, and for some species at least, remain active in anoxic conditions. In this  
84 context, several observational studies have shown foraminiferal survival after exposure to anoxia  
85 together with free sulphides (e.g., Langlet et al., 2013; 2014, Richirt et al., 2020), a combination  
86 which until recently was generally considered lethal (Moodley et al., 1998). The ultimate  
87 disappearance of benthic foraminifera during cases of long-term anoxia, as is for instance observed  
88 in Mediterranean sapropels (e.g., Jorissen, 1999b), seems therefore not to be the consequence of

89 strongly increased mortality, but rather of an inhibition of reproduction under strongly adverse  
90 conditions (Richirt et al., 2020).

91 These recent advances suggest that oxygen may not be the foremost environmental parameter  
92 explaining foraminiferal ecology, as was often thought in the past (e.g., Bernhard, 1886; Alve and  
93 Bernhard, 1995), and was more or less hypothesized in the TROX model. Instead, it appears that it is  
94 rather the quantity, and especially the quality of the food particles, which are the predominant  
95 parameters. However, the quality of the organic matter ( $C_{org}$ ) flux will also affect the biological  
96 oxygen demand, and thereby the bottom water and sediment redox conditions, so that the  
97 combination of the organic matter flux and oxygen content forms an inextricable complex.

98 Despite the determinant role of the organic matter flux, oxygen will still be a principal controlling  
99 factor when values are close to (or below) the tolerance levels of many species and/or higher  
100 taxonomical categories. Although alternative metabolic pathways for organic matter decomposition  
101 can be utilized under suboxic and anoxic conditions, they are energetically much less favourable,  
102 with the exception of denitrification (Froelich et al., 1979; Middelburg, 2019).

103 Furthermore, we have indications that the presence of free sulphides is not directly lethal (Bernhard  
104 et al., 1993; Langlet et al., 2014), but that long-term exposure leads to a decrease of foraminiferal  
105 population densities (Moodley et al., 1998; Richirt et al., 2020). It has been suggested that this would  
106 be due to a decrease of metabolic rate, and a loss of vital functions, such as growth, and especially  
107 reproduction (Moodley et al., 1998; Richirt et al., 2020). Long-term exposure to dissolved sulphides  
108 should therefore ultimately lead to the disappearance of foraminifera.

109

110 Summarising, even if our ideas about the specific role of some environmental factors, such as oxygen  
111 availability, have become more nuanced, the importance of redox conditions within the foraminiferal  
112 microhabitat remains paramount, and consequently, the conceptual TROX model (Jorissen et al.,  
113 1995) still provides an excellent tool to understand foraminiferal distribution patterns.

114

115 In this paper, we present a first attempt to translate the conceptual TROX-model into a numerical  
116 model, combining sediment early diagenesis (the combination of biological, chemical, and physical  
117 processes which change the quantity and composition of the organic matter in marine sediments  
118 before they become consolidated; Henrichs, 1992) and foraminiferal ecology.

119

120 The main aim of such a model is that it will allow us to test hypotheses concerning foraminiferal  
121 ecology. We will define theoretical species, with distinct characteristics, that each represent a group  
122 of real species with a similar microhabitat. We will then see how these theoretical species behave  
123 (are distributed) in the vertical succession of redox zones reproduced by the model, and compare the  
124 model results with observational data. If the model is capable of successfully reconstructing the field  
125 observations, this means that the underlying hypotheses concerning the foraminiferal ecology may  
126 be realistic. If this is not possible, the way the foraminiferal species are defined is probably incorrect.  
127 Ultimately, the aim is to use this model as a tool to test paleoceanographical scenarios and to  
128 reconstruct environmental parameters from foraminiferal successions in fossil records.

129

130 For the construction of the model, we profit from an extremely favourable context. First, early  
131 diagenetic models have become widely available. We decided to use the OMEXDIA model of Soetaert  
132 et al. (1996), which is well established, very well documented (Soetaert and Hermann, 2009) and  
133 freely available on the Comprehensive R Archive Network (<https://cran.r-project.org>). The OMEXDIA  
134 model will be coupled to a new foraminiferal model developed in the present study. Next, we employ  
135 a very large mixed database of sediment geochemistry (Anschutz et al., 1999, 2005; Hyacinthe et al.,  
2001, Chaillou et al., 2002, 2003, 2006; Mouret et al., 2009, 2010; Schmidt et al., 2009) and

135 foraminiferal distribution (Fontanier et al., 2002, 2003, 2005, 2006a; Langezaal et al., 2006; Mojtahid  
136 et al., 2010) for the Bay of Biscay. We decided to use the data collected between 1997 and 2001,  
137 when a bathymetrical transect from 150 to 2000 m water depth was sampled 10 times. This data set  
138 gives ample insight into seasonal and interannual variability of sediment geochemistry and  
139 foraminiferal communities. We will use this very large dataset to calibrate the model, and to test it in  
140 two different ecological settings.

141 This paper presents the first results of this exercise, in which the numerical model is developed, and  
142 is manually tested and tuned at two sampling stations, at 1000 and 550 m depth in the Bay of Biscay.  
143 In the process of developing the model, we sequentially tested a range of hypotheses regarding the  
144 benthic environment and its link to foraminiferal ecology. To illustrate the value of quantitative  
145 models for such hypothesis testing, we present this study in a manner that emphasizes the  
146 sequential steps in model development and calibration, highlighting the lessons learned along the  
147 way.

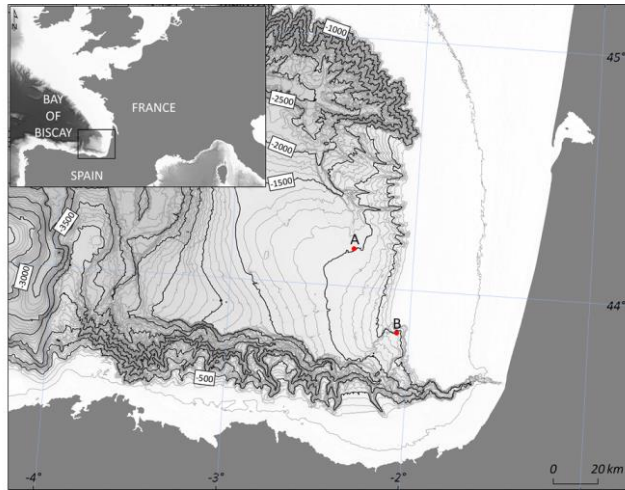
## 148 **2. Model characteristics**

149 When we set out to develop the coupled early diagenesis – benthic foraminiferal ecology model  
150 presented here, we chose to implement the model in the software R (R Core Team, 2020). R is widely  
151 used for scientific programming, and is freely available (<https://www.r-project.org>). We decided to  
152 use the early diagenetic model (1D) of Soetaert, which has been described in a number of  
153 publications (Soetaert et al., 1996; Soetaert & Herman, 2009), and is freely available online in the R-  
154 package ‘ReacTran’ (Soetaert and Meysman, 2012; [http://](http://www.rforscience.com/modelling/omexdia/)  
155 [www.rforscience.com/modelling/omexdia/](http://www.rforscience.com/modelling/omexdia/)).

156 The next step was to introduce theoretical species of benthic foraminifera, with different ecological  
157 characteristics (each theoretical species represents a group of real species), into this 1D geochemical  
158 environment. At a first stage, we investigated the possibility of constructing a quantitative biological  
159 model, including the most important life functions (e.g., growth, reproduction, mortality, etc.) of the  
160 different species. However, it soon turned out that this approach was severely hampered by a lack of  
161 observational data for most of these parameters. For this reason, we decided to change our strategy,  
162 and instead developed a “transformation model”, in which a fraction of the available resources was  
163 allocated to different members of the benthic foraminiferal community. More precisely, we assigned  
164 different proportions of the various types of organic matter ( $C_{org}$ ), more or less reactive, to the  
165 foraminiferal species introduced into the model.

166 We then tested the model on our extensive geochemical and foraminiferal dataset from the Bay of  
167 Biscay. After constructing the essential components of the model, we started to tune the model  
168 using the data of stations A and B, at 1000 and 550 m depth, respectively. We first optimized the fit  
169 between the geochemical data and the model results. Next, we tested various hypothesis concerning  
170 the ecological requirements of the benthic foraminifera, in order to obtain a maximum resemblance  
171 between observational data and model output.

172  
173  
174  
175  
176  
177  
178  
179  
180  
181  
182  
183



184 Fig. 1. Map of the bay of Biscay, with sampling stations A (1000 m) and B (550 m).

### 185 3. The Bay of Biscay data set

186 Bay of Biscay Stations A, at 1000 m water depth, and B, at 550 m depth, were visited 15 times  
187 between October 1997 and February 2011. The surficial sediment was sampled with an interface  
188 multi-corer, which allowed sampling the upper few decimetres of the sediment, the overlying  
189 bottom water, and the undisturbed sediment-water interface, in a 10 cm diameter Plexiglas tube. At  
190 both stations, very similar profiles of redox reactive compounds were measured in the numerous  
191 short cores collected over the 14 year interval (Mouret et al., 2016). Only small differences were  
192 noticed at the sediment surface, which were attributed to seasonality, bioturbation and/or spatial  
193 patchiness. For the present study we decided to concentrate on the period between October 1997  
194 and September 2001, when these stations were sampled 10 times, so that the seasonal and  
195 interannual variability of the geochemical composition of bottom and pore waters, as well as of the  
196 foraminiferal community, is particularly well constrained. The pore water geochemistry of these  
197 station has been described in detail by Hyacinthe et al. (2001), Anschutz et al. (2005), Mouret et al.  
198 (2009, 2010) and Charbonnier et al. (2019). Schmidt et al. (2009) concentrated on the particle fluxes  
199 and sediment accumulation rate. The foraminiferal community at the two stations was described by  
200 Fontanier et al. (2002; 2003; 2006a) and Mojtahid et al. (2010). Important seasonal and interannual  
201 variability was observed for the foraminiferal density and species composition. It appears that  
202 foraminiferal densities increased to an order of magnitude after major spring and autumn  
203 phytoplankton blooms, which favoured a limited number of opportunistic benthic foraminiferal taxa  
204 (Fontanier et al., 2003; 2006a).

205 In view of the observed stability of the succession of sediment redox zones (Mouret et al., 2009), we  
206 decided to use an averaged geochemical data set to calibrate our diagenetic model. To this purpose,  
207 for every geochemical model parameter, the observations for all available sampling campaigns (their  
208 number varied for different parameters) were averaged, so that a single value was obtained for all  
209 depth levels down to 10 cm depth in the sediment. For this first modelling study, foraminiferal data  
210 were averaged as well, for the 10 successive sampling campaigns.

#### 211 4. Early Diagenesis Model Parameters

212 The first portion of our model utilizes OMEXDIA, a reactive transport model for evaluating  
213 sedimentary diagenesis (Soetaert et al., 1996), which was run to steady state. It includes multiple  
214 organic matter remineralization pathways, incorporates key diagenetic chemical reactions, and  
215 allows for depth-dependent bioturbation/biodiffusion and porosity. In the present study, many of  
216 the key parameters of the model are constrained by observations derived from prior studies of  
217 stations A and B. Using the dataset of stations A and B, the model was manually tuned to provide  
218 initial constraints for the complete model, discussed later. The values of the main parameters used  
219 as starting point for the early diagenesis part of the model were the following:

- 220 • The organic carbon flux ( $C_{org}$ ) to the sea floor: for the 1000 m deep station A, Mouret et al.  
221 (2010) estimated a total  $C_{org}$  flux of  $16.5 \text{ gC m}^{-2} \text{ yr}^{-1}$ , consisting of 76% labile particulate  
222 organic carbon (POC), 9% slowly decaying POC, and 15% inert POC. At the 550 m deep  
223 station B, Mouret et al. (2010) estimated a total  $C_{org}$  flux of  $28.2 \text{ gC m}^{-2} \text{ yr}^{-1}$ , with 53.6% labile  
224 POC, 20.4% slowly degrading POC and 26.0% inert POC. These values were used as the basis  
225 for our tuning exercise. The most labile fraction was deduced from modelled dissolved  
226 oxygen consumption at the sediment surface. Other fractions were deduced from  $C_{org}$   
227 concentrations and mass accumulation rates.
- 228 • Bottom water temperature was always  $9.5^\circ\text{C}$  at station A, and  $11.0^\circ\text{C}$  at station B, without  
229 any seasonal variability (Ogawa et al., 1973; Durrieu de Madron et al., 1999 and Fontanier et  
230 al., 2006b).
- 231 • Bottom water oxygenation varied between  $189$  and  $201 \mu\text{mol l}^{-1}$  at station A and between  
232  $205$  and  $221 \mu\text{mol l}^{-1}$  at station B (Mouret et al., 2010; Anschutz and Chaillou; 2009).
- 233 • At both stations A and B, the sediment was a silty clay, with a mean grain size of  $5\text{--}6 \mu\text{m}$  at  
234 station A and  $10\text{--}15 \mu\text{m}$  at station B (Charbonnier et al., 2019). The sediment contained about  
235 30%  $\text{CaCO}_3$  at station A, versus 10–15% at station B. At both stations, sediment porosity  
236 decreased quickly in the first millimeters of the sediment, from 0.85 at the sediment-water  
237 interface to about 0.8 at 1 cm depth. Deeper down, porosity continued to decrease, until  
238 values between 0.65 and 0.7 were observed at 10 cm depth at stations A and B, respectively.
- 239 • The oxygen penetration depth into the sediment varied from 1.6 to 2.2 cm at station A, and  
240 from 1.1 to 1.9 cm at station B (Fontanier et al., 2003; 2006a; Mouret et al., 2010).
- 241 • At station A, nitrate in the bottom waters, sampled in the supernatant water of the sediment  
242 cores, varied from  $8.6$  to  $21.1 \mu\text{mol l}^{-1}$ , with a mean value of  $14.3 \mu\text{mol l}^{-1}$ . At station B,  
243 nitrate varied from  $11.5$  to  $15.7 \mu\text{mol l}^{-1}$ , with a mean value of  $14.1 \mu\text{mol l}^{-1}$ . These values are  
244 very close to those measured on water column samples taken with Niskin bottles (Anschutz  
245 and Chaillou, 2009). Maximum nitrate concentrations were generally observed in the top 2  
246 cm of the sediment, with values of  $24$  to  $33 \mu\text{mol l}^{-1}$  at station A, and  $19$  to  $23 \mu\text{mol l}^{-1}$  at  
247 station B. Deeper down, nitrate concentrations strongly decreased, with values below  $23$   
248  $\mu\text{mol l}^{-1}$  reached between 4 and 5 cm at station A and around 2 cm at station B. Ammonia  
249 always showed a strong downward increase from values around zero at the surface to mean  
250 values of  $30.7 \mu\text{mol l}^{-1}$  (station A) and  $61.1 \mu\text{mol l}^{-1}$  (station B) at 10 cm depth.
- 251 • Among the reduced components, dissolved  $\text{Mn}^{2+}$  and  $\text{Fe}^{2+}$  were only determined for part of  
252 the 10 sampling campaigns (Mouret et al., 2009), whereas no data for S(-II) were available.  
253 The sulphate concentration was constant with depth and equal to the  $\text{SO}_4^{2-}$  concentration in  
254 seawater. No sulphide smell was evident during core processing, but a few black patches  
255 were observed near the base of the cores, suggesting  $\text{H}_2\text{S}$  production in deeper sediment  
256 layers (Chaillou et al. 2003). Since the  $\text{H}_2\text{S}$  concentration was not measured, the model  
257 output for ODU (oxygen demand units, i.e. the amount of oxygen necessary to reoxidize

258 reduced counterparts from anaerobic mineralization), which regroups all reduced  
259 components, was always higher than the observations, which include only measured  
260 dissolved Mn and Fe.

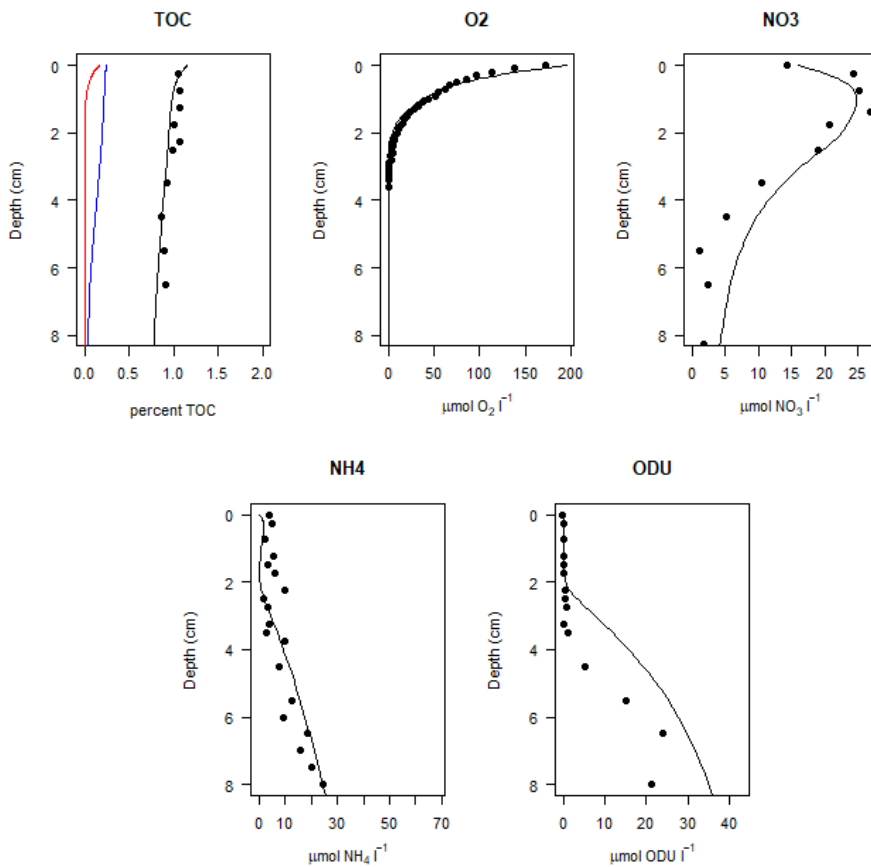
- 261 • At station A, the maximum sediment accumulation rate was estimated on the basis of  $^{210}\text{Pb}$   
262 profiles at 0.068 cm/year ( $36 \text{ mg cm}^{-2} \text{ yr}^{-1}$ ) by Chaillou et al. (2002), at 0.05 to 0.06 cm/year  
263 by Schmidt et al. (2009), whereas Mouret et al., 2009 obtained a value of 0.062 cm/year  
264 based on steady state manganese diagenesis. For station B, Chaillou et al. (2002) obtained a  
265 maximum sedimentation rate of 0.15 cm/year ( $79.5 \text{ mg cm}^{-2} \text{ yr}^{-1}$ ), compared to values of 0.12  
266 and 0.22 cm/year by Schmidt et al. (2009), and 0.12 cm/year based on steady state  
267 manganese diagenesis (Mouret et al., 2009).
- 268 • Mouret et al. (2009) obtained a large variety in biodiffusion coefficients, using  $^{234}\text{Th}$  profiles,  
269 for sediment cores sampled during four different campaigns, with values varying between  
270 0.12 and  $6.7 \text{ cm}^2/\text{year}$  at station A, and between 0.4 and  $14.8 \text{ cm}^2/\text{year}$  at station B. They  
271 estimated a mixed layer depth of about 1cm at both stations, slightly less than the depth of  
272 the oxic layer.

273 Despite the lack of observational data for some parameters (such as sulphur) in some of the  
274 cores, and the large variability observed for biodiffusion coefficients, the Bay of Biscay dataset  
275 for these two stations is remarkable by its near completeness for 10 successive sampling  
276 campaigns. It therefore forms an ideal dataset to develop and test our early diagenetic model.  
277 The main parameter that we used to tune the model was the  $C_{\text{org}}$  flux to the sea floor, or more  
278 precisely the proportions and reactivity constants of the various types of organic matter. A  
279 secondary main tuning parameter was the rate of pyrite formation in the sediment; this process  
280 withdraws reduced components from the pore water.

281

282 **5. Initial tuning of the preliminary (3G) early diagenetic model, using the station A data set**

283 Before introducing theoretical foraminiferal species into the model, our first objective was to tune  
284 the early diagenetic model to obtain an optimal fit between the averaged observed data and the  
285 model output. For this initial tuning exercise, we used the dataset for station A. Fig. 2 gives an  
286 example of an early result that employed three types of organic matter (3G).



287  
288  
289  
290  
291  
292  
293  
294  
295  
296  
297

298 Fig. 2. Station A - Model output for early diagenetic parameters (lines) of a preliminary version of the 4GFOR  
299 model, with only three types of organic matter (percent TOC = particulate  $C_{org}$  in weight % of dry sediment; red:  
300 fast degrading, blue: intermediate, black: total organic carbon (= fast degrading + intermediate + fossil),  
301 compared to observational data from Station A (dots).

302 It can be seen that the model results for  $C_{org}$ , oxygen and ammonia are very close to the observed  
303 data. However, although the modelled ODU curve has the right form, the absolute values are much  
304 higher than the observed ones. As explained in the previous section, this is likely due to the fact that  
305 only Fe and Mn were measured, and not S, a third major component contributing to ODU. As we do  
306 not intend to use ODU as a limiting factor for the foraminiferal species, we do not consider this very

307 important. The main problem with this preliminary model is the nitrate curve, which in deeper  
308 sediment layers shows values that are too high compared to the observed ones. This is important,  
309 because we intend to use a minimum  $\text{NO}_3^-$  concentration as a switch for nitrate-respiring  
310 foraminifera in the subsequent foraminiferal component of the model. All our attempts to improve  
311 the fit for nitrate systematically resulted in an upward movement of the oxygen profile, which is even  
312 more problematic, because we intended to use oxygen concentration as a switch for obligate aerobic  
313 foraminiferal species. In the final version of the model we resolved this problem by adding an  
314 additional diagenetic pathway, ferrous iron nitrification. This reaction, the anaerobic oxidation of  $\text{Fe}^{2+}$   
315 by nitrates (e.g., Straub et al., 1996; Kappler et al., 2021), appears to be an important process at our  
316 sites in the Bay of Biscay (Hyacinthe et al., 2001), and was hitherto not included in the OMEXDIA  
317 model. This early diagenetic pathway consumes nitrate at the lower part of its range, and diminishes  
318 ODU. After adding this reaction to the early diagenetic part of the model, we arrived at excellent fits  
319 for all parameters except ammonia, which was overestimated (Fig. 5). Since ammonia has no impact  
320 on the faunal distribution, this was considered less important.

## 321 6. Defining the foraminiferal species

322 As explained before, we decided not to include a fully biological model for the foraminiferal species,  
323 but rather a transformation model. This transformation model has two basic characteristics. First,  
324 foraminiferal activity is limited by critical environmental factors, such as oxygen and nitrate content.  
325 Beyond the critical threshold values, specified foraminifera are no longer given access to the  
326 available resources. Next, when these limiting factors are within the tolerance limits of the organism,  
327 a specific proportion of each type of  $C_{\text{org}}$  is attributed to each of the species. In the way we defined  
328 them, species living close to the sediment surface use a large proportion of reactive  $C_{\text{org}}$ , whereas  
329 species living deeper in the sediment use a larger proportion of slowly degrading  $C_{\text{org}}$ . This  
330 interspecific difference is based on two assumptions: 1) that infaunal foraminiferal taxa are better  
331 capable than surface dwellers to feed on organic matter of a lower quality, and 2) that sediment  
332 surface dwellers are more competitive than infaunal taxa when the uptake of high quality (highly  
333 reactive)  $C_{\text{org}}$  is concerned.

334 The allocation of different proportions of various qualities of organic carbon to different species is  
335 reminiscent of the BFAR-concept of Herguera and Berger (1991). In fact, Herguera and Berger  
336 assumed that for every mg of  $C_{\text{org}}$  arriving at the sea floor, roughly one foraminiferal shell  $> 150 \mu\text{m}$   
337 would be preserved in the sediment record.

338 In our first attempts to model the foraminiferal distribution in the sediment (for station A), we used a  
339 3G diagenetic model, with fast, slowly degrading, and inert  $C_{\text{org}}$ ; a very good fit between model  
340 output and observed data was obtained with decay rates  $r_{\text{fast}} = 0.01/\text{day}$ ,  $r_{\text{slow}} = 0.00005/\text{day}$  and  $r_{\text{fossil}} = 0$ . In these first runs (Fig. 3), we introduced only 2 foraminiferal species:

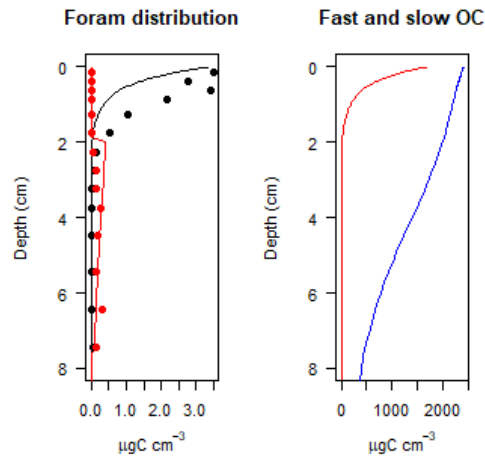
342 1) an epifaunal/shallow infaunal species, which was dependant on the presence of oxygen, at least at  
343 very low concentrations ( $\text{O}_2 > 2.5 \mu\text{mol l}^{-1}$ ). We defined this species group so that it exclusively feeds  
344 on fast decaying  $C_{\text{org}}$ .

345 2) a deep infaunal species, which we inhibited by oxygen ( $\text{O}_2 \leq 2.5 \mu\text{mol l}^{-1}$ ), but which was dependent  
346 on the presence of nitrate ( $\text{NO}_3^- > 2.5 \mu\text{mol l}^{-1}$ ), and given access to both fast and slowly degrading  
347  $C_{\text{org}}$ .

348 In order to compare the model outcome (in  $\text{mgC cm}^{-3}$ ) with the observational data (observed number  
349 of tests  $> 150 \mu\text{m}$ ), we assumed that a single foraminiferal individual ( $> 150 \mu\text{m}$ ) of the  
350 epifaunal/shallow infaunal species would contain  $0.625 \mu\text{g } C_{\text{org}}$ , whereas a deep infaunal individual ( $>$

351 150  $\mu\text{m}$ ) would on average contain 3.6  $\mu\text{g C}_{\text{org}}$ . These foraminiferal  $\text{C}_{\text{org}}$  contents are based on the  
 352 relationship between biovolume and protein content observed by Movellan et al. (2012), assuming  
 353 an average size of 250  $\mu\text{m}$  for epifaunal/shallow infaunal taxa (considered as semi-spheres,  
 354 representative of most epifaunal and trochospiral taxa) and of 450  $\mu\text{m}$  for deep infaunal taxa  
 355 (considered as a cylinder, such as *Globobulimina* spp.).

356  
357  
358  
359  
360  
361  
362  
363  
364  
365  
366



367 Fig. 3. First results of the coupled 3G early diagenesis (using two types of reactive organic matter) -  
 368 foraminiferal model. Left panel: epifaunal/shallow infaunal taxa (black) and deep infaunal taxa (red). Right  
 369 panel: fast degrading  $\text{C}_{\text{org}}$  (red) and intermediate degrading  $\text{C}_{\text{org}}$  (blue) Dots = observed data for station A (1000  
 370 m depth); lines = model output. Epifaunal/shallow infaunal taxa (black curve) only have access to fast decaying  
 371 organic matter.

### 372 7. Further developing the (3G) early diagenesis – perfecting the foraminiferal model for 373 station A

374 The first results of the coupled early diagenesis-foraminifera model for the 1000 m deep station A  
 375 (Fig. 3) were encouraging. To arrive at this fit, we attributed 0.2% of fast decaying  $\text{C}_{\text{org}}$  to  
 376 epifaunal/shallow infauna (when  $\text{O}_2 > 2.5 \mu\text{mol l}^{-1}$ , left panel, black curve), and 0.1% of fast decaying  
 377  $\text{C}_{\text{org}}$  and 0.002% of slowly degrading  $\text{C}_{\text{org}}$  to deep infauna (when  $\text{O}_2 \leq 2.5 \mu\text{mol l}^{-1}$  and  $\text{NO}_3 > 2.5 \mu\text{mol l}^{-1}$ , left panel, red curve).  
 378

379 These values, which were selected to obtain a reasonable fit, are in reality thought to reflect the  
 380 capacity of these species to feed on various types of  $\text{C}_{\text{org}}$ , and their competitive success compared to  
 381 other (foraminiferal as well as non foraminiferal) organisms feeding on the same resources. For  
 382 comparison, for continental shelf (37-60 m depth) and upper slope (450 m depth) environments with  
 383 well oxygenated bottom waters, Geslin et al. (2011) estimated the total foraminiferal contribution to  
 384 dissolved oxygen utilisation at 0.5 to 2.5%.

385 However, although the obtained result (Fig. 3) was encouraging, it was not yet fully acceptable.  
 386 There were in fact three major problems. The first problem was that the epifaunal/shallow infaunal  
 387 taxon did not penetrate deep enough into the sediment; their strong decline in the first cm of the  
 388 sediment is the direct consequence of the similar decline of the fast degrading  $\text{C}_{\text{org}}$  (red curve in the  
 389 right panel of fig. 3). In our opinion, the model results clearly show, that our initial hypothesis, that

390 epifaunal/shallow infaunal taxa exclusively feed on fast degrading  $C_{org}$ , is not supported. We solved  
391 this problem by attributing also a small fraction (0.004%) of slowly degrading  $C_{org}$  to  
392 epifaunal/shallow infaunal species (Fig. 4).

393

394

395

396

397

398

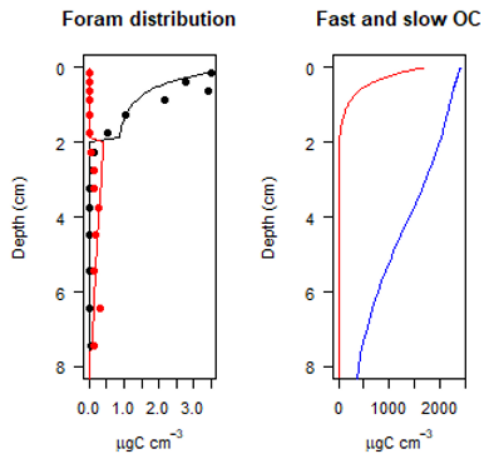
399

400

401

402

403



404 Fig. 4. First results of the coupled (3G) early diagenesis (using three types of organic matter) - foraminiferal  
405 model for station A (1000 m depth). Left panel: epifaunal/shallow infaunal taxa (black) and deep infaunal taxa  
406 (red). Right panel: fast degrading  $C_{org}$  (red) and intermediate degrading  $C_{org}$  (blue). Dots = observed data; lines =  
407 model output. Epifaunal/shallow infaunal taxa now have also access to a small part of slowly degrading  $C_{org}$ .

408 The second problem was the fact that in reality, there are more than two groups of foraminiferal  
409 species. There are not only deep infaunal species (such as *Globobulimina* spp.), but also intermediate  
410 infaunal species, such as *Melonis barleeanus*, which always attain the highest density at the depth  
411 where nitrate concentration is maximal (e.g., Jorissen et al., 1998). In addition, the group of  
412 epifauna/shallow infauna seems to be more complex, with some taxa always living close to the  
413 sediment-water interface, and others living slightly deeper in the oxygenated part of the surficial  
414 sediment. The first group is dominated by trochospiral genera (*Cibicidoides*, *Gyroidina*, *Hoeglundina*,  
415 *Oridorsalis*, etc.), whereas the second group is rather dominated by triserial and biserial genera  
416 (*Bolivina*, *Bulimina*, *Trifarina*, *Uvigerina*, etc.).

417 In order to take into account this complexity, we decided to expand our model to four theoretical  
418 foraminiferal taxa, each of which is supposed to represent a group of real species with similar  
419 microhabitat characteristics. Since we think that the name “epifauna” should be reserved for taxa  
420 living on elevated substrates above the sediment, we will use the terms “shallow infauna A” (SIA),  
421 “shallow infauna B” (SIB), “intermediate infauna” (II) and “deep infauna” (DI) for our four theoretical  
422 species (groups) living at increasingly greater depth in the sediment.

423 In order to model the vertical distribution of these four theoretical species, it soon turned out that a  
424 rough subdivision of the organic carbon resources into three types (fast degrading, slowly degrading,  
425 fossil) was insufficient. For this reason, we shifted to the final 4G model, with three types of reactive  
426  $C_{org}$ : fast, intermediate and slowly degrading, and finally inert  $C_{org}$ .

427 The final problem was that in the first versions of the model (Figs. 3, 4), we inhibited the activity of  
428 the deep infaunal species with oxygen. However, Nomaki et al. (2007) observed oxic respiration for

429 the deep infaunal taxa *Globobulimina affinis* and *Chilostomella ovoidea*. Consequently, in most  
430 studies, deep infaunal taxa are considered as facultative anaerobes, which will only shift to an  
431 anaerobic metabolism (using nitrate) when no oxygen is available.

432 We solved this problem by replacing the inhibition with an additional scaling factor. In fact, we  
433 defined the intermediate and deep infaunal categories in such a way that the amount of fast and  
434 intermediate degrading  $C_{org}$  allocated to them decreases exponentially towards higher oxygen  
435 concentration. In biological terms, this means that these taxa become rapidly less competitive  
436 (compared to shallow infaunal groups A and B) when oxygen concentrations increase. In our opinion,  
437 this is a very realistic way to define these species for the sake of our quantitative model.

#### 438 **8. Tuning the final 4GFOR Model for stations A (1000 m) and B (550 m).**

439 Concerning the final tuning of the early diagenesis part of the 4GFOR model, an optimal fit between  
440 model output and observations was obtained by using a total  $C_{org}$  flux of 16.0 and 25.0  $gC\ m^{-2}\ yr^{-1}$  at  
441 stations A and B, respectively (table 1). These values are very close to the values of 16.5 and 28.2  $gC$   
442  $m^{-2}\ yr^{-1}$  given by Mouret et al., 2010).

Parameter	Description	Station A	Station B	Unit	Source
maxdep	Maximum depth for modeled sediment	24	24	cm	I
pO	Porosity in surface sediment	83.3	88.5	%	I
pinf	Porosity at maximum modeled depth	64.2	69.7	%	I
pco	Coefficient of decrease for porosity	4.47	2.76		I
sedr	Sedimentation rate	0.055	0.15	cm/year	L <sup>6</sup>
Db	Bioturbation rate	0.75	1.25	cm/year	L <sup>3</sup>
mixl	Mixed layer depth	1.0	1.0	cm	L <sup>3</sup>
fluxm	Total Corg flux at sediment water interface	16.0	25.0	g m <sup>-2</sup> y <sup>-1</sup>	L <sup>3</sup> ; C
TCorginf	%Corg at infinite depth	0.79	0.83	%	L <sup>3</sup>
rfast	1st order rate constant for fast degrading Corg	0.026	0.015	day <sup>-1</sup>	C
rint	1st order rate constant for intermediately degrading Corg	0.001	0.0005	day <sup>-1</sup>	C
rslow	1st order rate constant for slowly degrading Corg	0.00003	0.0000025	day <sup>-1</sup>	C
pfast	fraction of fast degrading Corg in total Corg flux	58.41	34.0	%	C
pint	fraction of intermediate degrading Corg in total Corg flux	20.0	21.5	%	C
pslow	fraction of slow degrading Corg in total Corg flux	6.26	18.5	%	C
NCrFdat	NC ratio fast decay det	0.16	0.16	molN/molC	L <sup>5</sup> ; C
NCridat	NC ratio intermediate decay det	0.2	0.2	molN/molC	C
NCrSdat	NC ratio slow decay det	0.13	0.13	molN/molC	L <sup>5</sup>
Pdepo	Fraction of ODU production deposited as solid	0.44	0.44	% day <sup>-1</sup>	L <sup>5</sup>
Temp	Bottom water temperature	9.5	11	°C	L <sup>2,4</sup>
bwO2	Oxygen concentration in bottom water	196.5	213.4	mmol m-3	L <sup>3</sup> ; I
bwNO3	Nitrate concentration in bottom water	16	14	mmol m-3	L <sup>1</sup> ; I
bwNH3	Ammonia concentration in bottom water	0	0.6	mmol m-3	L <sup>1</sup> ; I
NH3bot	Ammonia conc at bottom modeled sediment column	68.29	200	mmol m-3	I
ksO2oxic	Half-saturation O2 in oxic mineralisation	30	30	mmol m-3	L <sup>5</sup>
ksNO3denit	Half-saturation NO3 in denitrif	15	15	mmol m-3	L <sup>5</sup>
kinO2denit	Half-saturation O2 inhib denitrif	0.5	0.5	mmol m-3	L <sup>5</sup>
kinNO3anox	Half-saturation NO3 inhib anoxic min	1	1	mmol m-3	L <sup>5</sup>
kinO2anox	Half-saturation O2 inhib anoxic min	5	5	mmol m-3	L <sup>5</sup>
ksO2nitri	Half-saturation O2 in nitrification	100	100	mmol m-3	L <sup>5</sup>
ksO2oduox	Half-saturation O2 in oxidation of ODU	100	100	mmol m-3	L <sup>5</sup>
rODUox	Maximum rate oxidation of ODU	20	20	day <sup>-1</sup>	L <sup>5</sup>
rnit	Maximum nitrification rate	20	20	day <sup>-1</sup>	L <sup>5</sup>
NH3Ads	Adsorption coefficient ammonium	1.3	1.3		L <sup>5</sup>
roxidNO3	Maximum oxidation of ODU by NO3	200	200	day <sup>-1</sup>	L <sup>5</sup>
ksNO3ODUox	Half-saturation NO3 in Fe oxydation	200	200	mmol m-3	L <sup>5</sup>
kinO2ODUox	Half-saturation O2 in Fe oxydation	1	1	mmol m-3	L <sup>5</sup>

443  
444 Table 1. Parameters used in the final simulation of the early diagenesis part of the 4GFOR model. The source of  
445 the parameter values is indicated as follows: C = constrained with the model using the measured data; I =  
446 independently determined from field data; L = based on literature values, retrieved from: <sup>1</sup>Anschutz and  
447 Chaillou (2009); <sup>2</sup>Durrieu de Madron et al. (1999); <sup>3</sup>Mouret et al. (2010); <sup>4</sup>Ogawa et al. (1973) ; <sup>5</sup>Soetaert et al.  
448 (1996) ; <sup>6</sup>Schmidt et al. (2009).

449 Compared to Mouret et al. (2010), the fractions of inert C<sub>org</sub> (0.153 and 0.26) were not changed. Of  
450 the 0.2 and 0.215 parts (stations A and B, respectively) attributed to the newly created category  
451 C<sub>org,nt</sub>, compared to the observations of Mouret et al. (2010), the large majority (87.5 and 91.2% for  
452 stations A and B) was taken from the labile C<sub>org</sub>, and the remaining part from the slowly decaying C<sub>org</sub>.

453 The presence of the four foraminiferal species was constrained with the boundary conditions listed in  
454 Table 2, which determined whether they were present or not. In our first attempts, using the data of  
455 station A, for deep infauna, we used a threshold value for nitrate of 2.5 μmol l<sup>-1</sup>. It turned out that at  
456 station B, where the nitrate concentration diminishes rapidly with greater depth in the sediment, this

457 threshold truncated the downward distribution of deep infauna. In order to better simulate our field  
 458 observations, we subsequently decreased the nitrate threshold for deep infauna to 0.05  $\mu\text{mol l}^{-1}$ .

459

460

461

462

463

	Oxygen	Nitrate
Shallow infauna A	>2.5 $\mu\text{mol l}^{-1}$	No nitrate limitation
Shallow infauna B	>2.5 $\mu\text{mol l}^{-1}$	No nitrate limitation
Intermediate infauna	No oxygen limitation	>2.5 $\mu\text{mol l}^{-1}$
Deep infauna	No oxygen limitation	>0.05 $\mu\text{mol l}^{-1}$

464 Table 2. Threshold values of oxygen and nitrate concentrations for the four theoretical species of benthic  
 465 foraminifera.

466 Finally, foraminiferal biomass was tuned to the observational data by changing the fractions of the  
 467 different types of  $C_{\text{org}}$  attributed to the four theoretical species of foraminifera, as shown in Table 3.

468

<b>Station A – 1000 m</b>	$C_{\text{orgfast}}$	$C_{\text{orgint}}$	$C_{\text{orgslow}}$
Shallow infauna A	0.0006	0.0006	0
Shallow infauna B	0.0003	0.0012	0
Intermediate infauna	0.0002	0.0004	0.00001
Deep infauna	0.0001	0.0001	0.00015

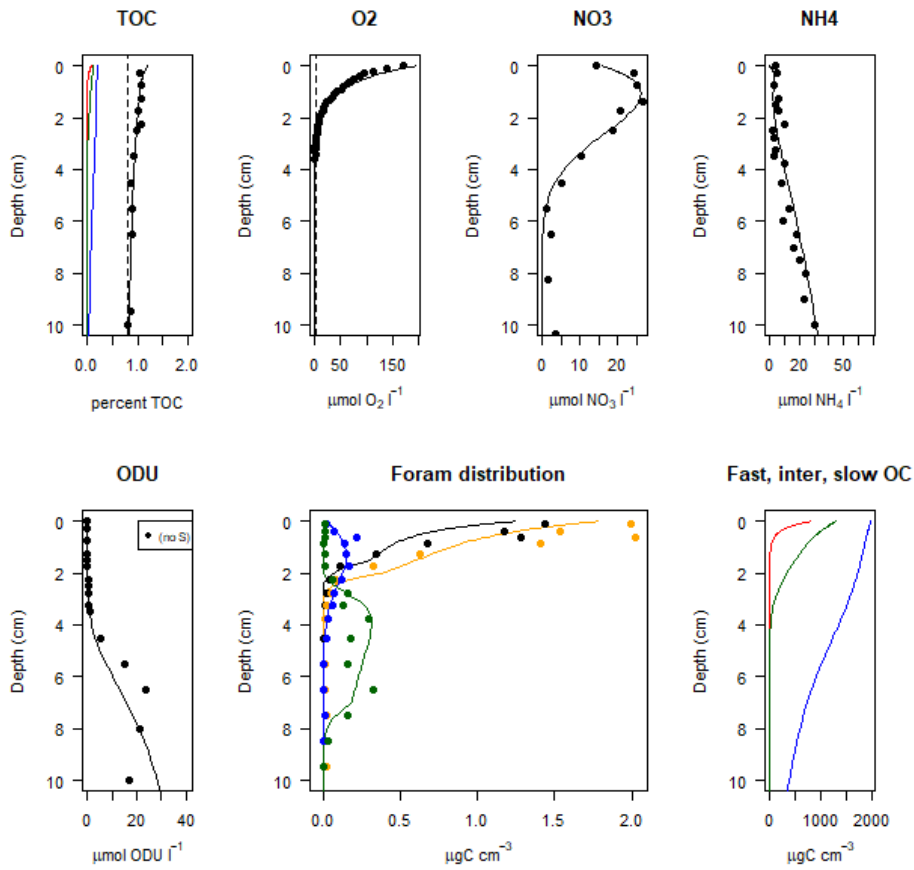
<b>Station B – 550 m</b>	$C_{\text{orgfast}}$	$C_{\text{orgint}}$	$C_{\text{orgslow}}$
Shallow infauna A	0.0006	0.0006	0
Shallow infauna B	0.0003	0.0012	0
Intermediate infauna	0.004	0.00033	0.00001
Deep infauna	0.0001	0.00001	0.00011

469

470 Table 3. Fractions of the three types of reactive organic carbon attributed to each of the 4 theoretical species of  
 471 foraminifera, at stations A and B.

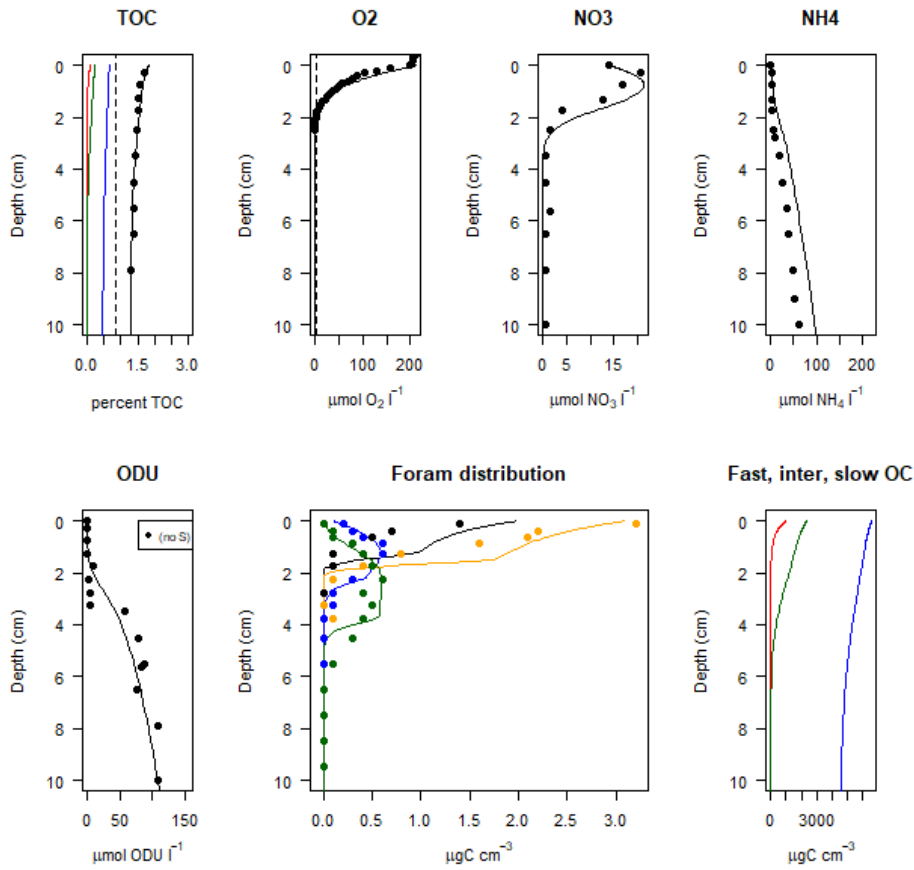
472 The competitiveness of intermediate infauna/deep infauna with respect to highly and intermediately  
 473 reactive  $C_{\text{org}}$  further depends on oxygenation: it is low/very low under oxic conditions, and high/very  
 474 high under hypoxic/anoxic conditions.

475 The final results of the tuning procedure of the 4GFOR model are shown in Figs. 5 and 6. As noted  
 476 earlier, the fit between the observed and modelled profiles of early diagenetic parameters is very  
 477 satisfactory. The two shallow infaunal species (A and B) are well separated in the top 1-2 cm of the  
 478 sediment, suggesting that our decision to differentiate them by their ability to cope with low quality  
 479  $C_{\text{org}}$  may be realistic. The profiles of intermediate and deep infaunal taxa correspond well with the  
 480 observed data, although in detail, the modelled distribution is slightly off for some levels.



481

482 Fig. 5. Final results for station A (1000 m depth) of the 4GFOR model with four types of organic matter (red:  
 483 fast degrading, green: intermediate, blue: slow, and black: total TOC). Foraminiferal species distribution is  
 484 represented as: Shallow Infauna A = black, Shallow Infauna B = orange, Intermediate Infauna = blue, Deep  
 485 Infauna = green. All dots are averaged observed data, lines are model output.



486  
 487 Fig. 6. Final results for station B (550 m depth) of the 4GFOR model with four types of organic matter (red: fast  
 488 degrading, green: intermediate, blue: slow, and black: total TOC). Foraminiferal species distribution is  
 489 represented as: Shallow Infauna A = black, Shallow Infauna B = orange, Intermediate Infauna = blue, Deep  
 490 Infauna = green. All dots are averaged observed data, lines are model output.

491 **9. Discussion**

492 **9.1. Definition of organic matter**

493 The organic matter flux to the seafloor is composed of a large variety of particles, such as living  
 494 microbial cells and secondary producers, detrital material, fecal pellets, other aggregates, and  
 495 continental organic matter, as well as of dissolved organic carbon (Middelburg, 2018). Consequently,  
 496 particulate organic matter has a wide range of components, such as inert carbon, lipids, amino acids,  
 497 vitamins and carbohydrates. These components have very different reactivities. In models this range  
 498 of organic matter can be represented in different ways, by two (2G), three (3G) or four (4G) groups  
 499 with different reactivity, or, in the most sophisticated models, by a continuous range of organic  
 500 matter quality (Arndt et al., 2013). In the first version of our model, we used a 3G approach, with  
 501 inert, reactive and less reactive Corg types, whereas in the last (4G) version we added an  
 502 intermediate category, which allowed us to obtain much better simulations of the observational  
 503 data.

504

## 505 9.2. Characteristics of foraminiferal species

506 While developing the 4GFOR model, the characteristics of our theoretical foraminiferal species have  
507 progressively evolved, to become more complex. In our first runs, we attributed only fast degrading  
508  $C_{org}$  to the shallow infaunal species. It turned out that because of the rapid decrease of  $C_{org-fast}$  with  
509 depth, compared to observational data, our model species did not penetrate deep enough into the  
510 sediment. This example emphasizes the great importance of theoretical models: apparently the basic  
511 hypothesis (= shallow infaunal taxa feed exclusively on  $C_{org-fast}$ ) was wrong, and consequently, the  
512 model was incapable of simulating the observed data.

513 We solved this problem by separating the group of shallow infaunal taxa into two species, SIA and  
514 SIB, with SIB being much more tolerant to lower quality  $C_{org}$  than SIA. The existence of two shallow  
515 infaunal groups with different dominant test forms (SIA = trochospiral, planispiral; SIB = biserial,  
516 triserial) is in accordance with abundant microhabitat observations in natural ecosystems and is  
517 corroborated by the interspecific differences in the  $\delta^{13}C$  of their shells (e.g., McCorkle et al., 1990;  
518 Rathburn et al., 1996; Fontanier et al., 2006b). By giving them access to different proportions of fast  
519 degrading and intermediate  $C_{org}$ , we could obtain a nearly perfect fit with the observed data.

520 In our first trials, we used only a single deeper infaunal taxon, and we forced this species to remain at  
521 depth in the sediment by limiting it to oxygen concentrations below  $2.5 \mu\text{mol l}^{-1}$ . In the later versions,  
522 we separated this group into intermediate and deep infaunal taxa, in accordance with the large  
523 volume of natural observations. Both groups were initially defined in such a way that they can only  
524 occur when nitrate concentration is above  $2.5 \mu\text{mol l}^{-1}$ . In order to obtain a deeper penetration of  
525 deep infauna at station B, we had to lower this threshold to  $0.05 \mu\text{mol l}^{-1}$  for this group. We further  
526 differentiated intermediate and deep infauna by making DI more tolerant to low quality  $C_{org}$  than II.  
527 To avoid that these species invade the superficial sediment layers, where large amounts of highly  
528 reactive  $C_{org}$  are present, we added a competitive element, by attributing less  $C_{org-fast}$  and  $C_{org-int}$  to  
529 these taxa when oxygen rises above  $2.5 \mu\text{mol l}^{-1}$ , with an exponential decrease towards higher  
530 oxygen levels. With these characteristics, the overall distribution of II and DI is very close to the  
531 observed patterns. This suggests that the way we defined these taxa may be correct, and that their  
532 absence in the superficial sediment layers may indeed be the consequence of a strongly diminished  
533 competitiveness in well oxygenated environments. In more general terms, this suggests that  
534 interspecific competition for food particles may be an important controlling parameter.

535 Finally, when tuning the model for two stations with very different characteristics, we managed to  
536 obtain a good fit for the early diagenesis parameters while using the same reaction constants at both  
537 stations. This underlines the robustness of this part of the model. In order to obtain good fits for the  
538 foraminiferal data at both stations, we had to attribute slightly different proportions of the different  
539 organic matter types to the four theoretical species (Table 3). This suggests that the foraminiferal  
540 contribution to organic matter remineralisation may change as a function of the environmental  
541 conditions.

## 542 9.3. Perspectives

543 Here, we present the newly developed 4GFOR model, and our tuning with the data of two sampling  
544 station at 1000 and 550 m depth in the Bay of Biscay, on the basis of averaged data of 10 successive  
545 sampling campaigns. In view of the obtained simulations, which are very close, both for geochemical  
546 as for foraminiferal species, it appears that the complexity of the model is enough to correctly  
547 represent the four main groups of foraminifera. The next step will be to test the model in different

548 environmental settings. We will accomplish this by modelling 1) the 10 successive sample times  
549 individually, 2) the 8 other stations of the Bay of Biscay transect, between 140 and 4800 m depth,  
550 with a wide range of environmental characteristics, 3) sampling stations from other ocean basins  
551 (Indian Ocean, Cape Blanc upwelling) from which we have comparable data sets. These modelling  
552 exercises will very probably lead to adjustments of the model, and the way the foraminiferal species  
553 are defined. This will oblige us to consider slightly different ecological strategies for the four species,  
554 and thereby, to test many hypotheses we still have regarding their life strategies.

555 Once the robustness of the 4GFOR model has been fully demonstrated, the next step will be to  
556 develop a formal inversion of the model, so that the main parameters controlling the foraminiferal  
557 faunas, the quantity and quality of the organic flux to the sea floor and the vertical succession of  
558 redox species, can be reconstructed on the basis of the composition of fossil faunas in sediment  
559 cores and outcrops.

## 560 **10. Conclusion**

561 The 4GFor model is a combination of an early diagenetic model, based on the OMEXDIA model of  
562 Soetaert et al. (1996), and a transformation model, which transforms proportions of organic matter  
563 types with different reaction rates into foraminiferal biomass. Foraminiferal communities are  
564 simulated with four theoretical deep water species. Their different tolerance levels with respect to  
565 oxygen and nitrate concentrations decide at what depths they can occur, whereas their density is  
566 mainly controlled by organic matter quality.

567 The model has been tuned to a large geochemical and foraminiferal database of two stations, at  
568 1000 and 550 depth in the Bay of Biscay. The outcome shows that the early diagenesis part of the  
569 model correctly reproduces the vertical distribution of redox species in the top 10 cm of the  
570 sediment. By attributing various proportions of the different types of organic matter to the four  
571 foraminiferal species, the model adequately reproduces the vertical succession of shallow,  
572 intermediate and deep infaunal species.

573 The model further separates shallow infaunal taxa into two groups. Group SIA, which is found close  
574 to the sediment-water interface, corresponds to trochospiral (e.g., *Cibicidoides*, *Gyroidina*,  
575 *Hoeglundina*) and planispiral species (e.g., *Cassidulina*). This group is critically sensitive to food  
576 quality. Group SIB, which is found slightly deeper in the sediment, corresponds to triserial (e.g.,  
577 *Bulimina*, *Uvigerina*) and biserial (e.g., *Bolivina*) taxa, which are less restrictive with respect to food  
578 quality. The observed distribution of these groups at the two stations in the Bay of Biscay is  
579 reproduced by the model. Also, the depth in the sediment of intermediate (e.g., *Melonis barleeanus*)  
580 and deep infaunal (e.g., *Globobulimina* spp.) species is very well simulated.

581 The tuning of the model indicates that shallow infaunal taxa (neither SIA nor SIB) do not feed  
582 exclusively on the most labile  $C_{org}$  component. Their vertical distribution can only be simulated by  
583 giving them access to slightly less reactive  $C_{org}$ .

584 One of the problems encountered during the tuning phase was to keep intermediate and deep  
585 infaunal taxa restricted to deeper layers. Because of the presence of large quantities of high quality  
586  $C_{org}$  close to the sediment surface, this layer is also attractive for those species. To solve this problem,  
587 we diminished their competitive ability exponentially towards higher oxygen levels. This solution  
588 appears to be realistic, but should be tested in experimental conditions.

589 As is shown by these first examples, the 4GFOR model can be a powerful tool to help understand  
590 foraminiferal ecology. In the future, we intend to construct a formal inversion of the model, which

591 will make it possible to produce quantitative estimates of the main controlling faunal parameters  
592 (quantity and quality of the organic flux, oxygen and nitrate concentration) on the basis of the  
593 composition of fossil foraminiferal assemblages.

#### 594 **11. Acknowledgements**

595 The authors are grateful to Karline Soetaert for her help with the addition of the ferrous iron  
596 nitrification reactions to the early diagenesis model.

#### 597 **12. References**

- 598 Alve, E., Bernhard, J.M., 1995. Vertical migratory response of benthic foraminifera to controlled  
599 oxygen concentrations in an experimental mesocosm. *Marine Ecology Progress Series*, 116, 137-151.
- 600 Anschutz, P., Chaillou, G., 2009. Deposition and fate of reactive Fe, Mn, P and C in suspended  
601 particulate matter in the Bay of Biscay. *Continental Shelf Research* 29, 1038-1043.
- 602 Anschutz, P., Dedieu, K., Desmazes, F., Chaillou, G., 2005. Speciation, oxidation state, and reactivity  
603 of particulate manganese in marine sediments. *Chem. Geol.*, 218, 265–279.
- 604 Anschutz, P., Hyacinthe, C., Carbonel, P., Jouanneau, J.M., Jorissen, F.J., 1999. The distribution of  
605 inorganic phosphorus in modern sediments of the Bay of Biscay. *C.R. Acad. Sci. Paris*, 328, 765-771.
- 606 Arndt, S., Jørgensen, B.B., LaRowe, D.E., Middelburg, J.J., Pancost, R.D., Regnier, P., 2013.  
607 Quantifying the degradation of organic matter in marine sediments: A review and synthesis. *Earth-  
608 Science Reviews*, 123, 53–86.
- 609 Bernhard, J.M., 1986. Characteristic assemblages and morphologies of benthic foraminifera from  
610 anoxic, organic-rich deposits: Jurassic through Holocene.
- 611 Bernhard, J.M., 1993. Experimental and field evidence of Antarctic foraminiferal tolerance to anoxia  
612 and hydrogen sulfide. *Marine Micropaleontology*, 20, 203-213.
- 613 Bernhard, J.M., Alve, E., 1996. Survival, ATP pool, and ultrastructural characterization of benthic  
614 foraminifera from Drammensfjord (Norway): response to anoxia. *Marine Micropaleontology*, 28, 5-  
615 17.
- 616 Bernhard, J.M., Bowser, S.S., 1999. Benthic foraminifera of dysoxic sediments: chloroplast  
617 sequestration and functional morphology. *Earth-Science Reviews*, 46, 149–165.
- 618 Bernhard, J. M., Casciotti, K. L., McIlvin, M. R., Beaudoin, D.J., Visscher, P. T., Edgcomb, V. P.,  
619 2012. Potential importance of physiologically diverse benthic foraminifera in sedimentary nitrate  
620 storage and respiration, *J. Geophys. Res.*, 117, G03002, doi:10.1029/2012JG001949, 2012.
- 621 Canfield, D.E., Jørgensen, B.B., Fossing, H., Glud, R., Gundersen, J., Ramsing, N.B., Thamdrup, B.,  
622 Hansen, J.W., Nielsen, L.P., Hall, P.O.J., 1993. Pathways of organic carbon oxidation in three  
623 continental margin sediments. *Mar. Geol.* 113, 27-40.
- 624 Carney, R. S., 2005. Zonation of deep biota on continental margins. *Oceanography and Marine  
625 Biology. Annual Review*, 43, 211–278.
- 626 Chaillou, G., Anschutz, P., Lavaux, G., Blanc, G., 2006. Rare earth elements in the modern sediments  
627 of the Bay of Biscay (France). *Mar. Chem.*, 100, 39–52.
- 628 Chaillou, G., Anschutz, P., Lavaux, G., Schäfer, J., Blanc, G., 2002. The distribution of Mo, U, and Cd  
629 in relation to major redox species in muddy sediments of the Bay of Biscay. *Mar. Chem.*, 80, 41–59.
- 630 Chaillou, G., Schäfer, J., Anschutz, P., Lavaux, G., Blanc, G., 2003. The behaviour of arsenic in  
631 muddy sediments of the Bay of Biscay (France). *Geochim. Cosmochim. Acta*, 67, 2993–3003.
- 632 Charbonnier C., Mouret A., Howa H., Schmidt S., Gillet H., Anschutz P. 2019. Quantification of  
633 diagenetic transformation of continental margin sediments at the Holocene time scale. *Continental  
634 Shelf Research*, 180, 63-74.
- 635 Corliss, B.H., 1985, Microhabitats of benthic foraminifera within deep-sea sediments: *Nature*, v. 314,  
636 p. 435-438.

637 Corliss, B.H., Chen, C., 1988, Morphotype patterns of Norwegian Sea deep-sea benthic foraminifera  
638 and ecological implications: *Geology*, v. 16, p. 716-719.

639 Corliss, B.H., Emerson, S., 1990. Distribution of Rose Bengal stained deep-sea benthic foraminifera  
640 from the Nova Scotian continental margin and Gulf of Maine. *Deep-Sea Research*, 37, 381-400.

641 Fontanier, C., Jorissen, F.J., Licari, L., Alexandre, A., Anschutz, P., Carbonel, P., 2002. Live benthic  
642 foraminiferal faunas from the Bay of Biscay; faunal density, composition and microhabitats. *Deep-Sea  
643 Research*, I, 49, 751-785.

644 Fontanier, C., Jorissen, F.J., Chaillou, G., David, C., Anschutz, P., Lafon, V., 2003. Seasonal and  
645 interannual variability of benthic foraminiferal faunas at 550 m depth in the Bay of Biscay. *Deep-Sea  
646 Research*, I, 50, 457-494.

647 Fontanier C., Jorissen F.J., Chaillou G., Anschutz P., Grémare A., Griveaud C., 2005. Live  
648 foraminiferal faunas from a 2800 m deep lower canyon station from the Bay of Biscay: Faunal  
649 response to focusing of refractory organic matter. *Deep-Sea Research*, I, 52, 1189-1227.

650 Fontanier, C., Jorissen, F.J., Anschutz, P., Chaillou, G., 2006a. Seasonal variability of benthic  
651 foraminiferal faunas at 1000 m depth in the Bay of Biscay. *Journal of Foraminiferal research*, 36, 61-  
652 76.

653 Fontanier, C., Mackensen, A., Jorissen, F.J., Anschutz, P., Licari, L., Griveaud, C. 2006b. Stable  
654 oxygen and carbon isotopes of live benthic foraminifera from the Bay of Biscay: Microhabitat impact  
655 and seasonal variability. *Marine Micropaleontology*, 58, 159-183.

656 Froelich, P.N., Klinkhammer, G.P., Bender, M.L., Luedke, N.A., Heath, G.R., Cullen, D., Dauphin, P.,  
657 Hammond, D., Hartman, B., Maynard, V., 1979. Early oxidation of organic matter in pelagic  
658 sediments of the Eastern Equatorial Atlantic: suboxic diagenesis. *Geochim. Cosmochim. Acta* 43,  
659 1075-1090.

660 Geslin, E., Risgaard-Petersen, N., Lombard, F., Metzger, E., Langlet, D., Jorissen, F.J., 2011. Oxygen  
661 respiration rates of benthic foraminifera as measured with oxygen microsensors. *Journal of  
662 Experimental Marine Biology and Ecology*, 396, 108-114.

663 Gooday, A.J., 1986. Meiofaunal foraminiferans from the bathyal Porcupine Seabight (northeast  
664 Atlantic): Size structure, standing stock, taxonomic composition, species diversity and vertical  
665 distribution in the sediment. *Deep-Sea Research*, 33, 1345-73.

666 Henrichs, S.M., 1992. Early diagenesis of organic matter in marine sediments: progress and  
667 perplexity. *Marine Chemistry*, 39, 119-149.

668 Herguera, J. C., Berger, W., 1991. Paleoproductivity from benthonic foraminifera abundance: Glacial  
669 to postglacial change in the west-equatorial Pacific. *Geology*, 19, 1173-1176.

670 Høglund, S., Revsbech, N.P., Cedhagen, T., Nielsen, L.P., Gallardo, V.A., 2008. Denitrification,  
671 nitrate turnover, and aerobic respiration by benthic foraminiferans in the oxygen minimum zone off  
672 Chile. *J. Exp. Mar. Biol. Ecol.*, 359, 85-91.

673 Hyacinthe, C., Anschutz, P., Carbonel, C., Jouanneau, J.M., Jorissen, F.J. 2001. Early diagenetic  
674 processes in muddy sediments of the Bay of Biscay. *Marine Geology*, 177, 111-128.

675 Jauffrais, T., Jesus, B., Metzger, E., Mouget, J.L., Jorissen, F., Geslin, E., 2016. Effect of light on  
676 photosynthetic efficiency of sequestered chloroplasts in intertidal benthic foraminifera (*Haynesina  
677 germanica* and *Ammonia tepida*). *Biogeosciences*, 13, 2715-2726.

678 Jorissen, F.J., 1999a. Benthic foraminiferal microhabitats below the sediment-water interface. In: Sen  
679 Gupta, B. (ed.): *Ecology of recent foraminifera*, Kluwer Academic Publishers, chapter 10, p. 161-179.

680 Jorissen, F.J., 1999b. Benthic foraminiferal successions across Late Quaternary Mediterranean  
681 Sapropels. *Marine Micropaleontology*, 153, 91-101.

682 Jorissen, F.J., De Stigter, H.C., Widmark, J.G.V. (1995) A conceptual model explaining benthic  
683 foraminiferal microhabitats. *Marine Micropaleontology*, 26, 3-15.

684 Jorissen, F.J., Fontanier, C., Thomas, E., 2007. Paleoceanographical proxies based on deep-sea benthic  
685 foraminiferal assemblage characteristics. In: Hillaire-Marcel, C., and De Vernal, A. (eds.): *Proxies in  
686 Late Cenozoic Paleoceanography*. Elsevier Publishers. *Developments in Marine Geology*, 1, 263-325.

687 Jorissen, F.J., Wittling, I., Peypouquet, J.P., Rabouille, C., Relexans, J.C., 1998. Live benthic  
688 foraminiferal faunas off Cap Blanc, NW Africa; community structure and microhabitats: Deep-Sea  
689 Research I, 45, p. 2157-2188.

690 Kappler, A., Bryce, C., Mansor, M., Byrne, J.M., Swanner, E.D., 2021. An evolving view on  
691 biogeochemical cycling of iron. *Nature reviews microbiology*, 19, 360-374.

692 Koho, K.A., De Nooijer, L.J., Reichart, G.J., 2015. Combining benthic foraminiferal ecology and shell  
693 Mn/Ca to deconvolve past bottom water oxygenation and paleoproductivity. *Geochim. Cosmochim.*  
694 *Acta*, 165, 294-306.

695 Langezaal, A.M., Jorissen, F.J., Braun, B., Chaillou, G., Fontanier, C., Anschutz, P., Van der Zwaan,  
696 G.J., 2006. The influence of seasonal processes on geochemical profiles and foraminiferal assemblages  
697 on the outer shelf of the Bay of Biscay. *Continental Shelf research*, 26, 1730-1755.

698 Langlet, D., Baa, C., Geslin, E., Metzger, E., Zuschin, M., Riedel, B., Risgaard-Petersen, N.,  
699 Stachowitsch, M., Jorissen, F.J., 2014. Foraminiferal species responses to in situ, experimentally  
700 induced anoxia in the Adriatic Sea. *Biogeosciences*, 11, 1775-1797.

701 Lee, J.J., Anderson, O.R., 1991. Symbiosis in Foraminifera. In: Lee, J.J., Anderson, O.R. (Eds.),  
702 *Biology of Foraminifera*. Academic Press, London, pp. 157-220.

703 Leutenegger, S., 1984. Symbiosis in benthic foraminifera: specificity and host adaptations. *J.*  
704 *Foraminiferal Res.*, 14, 16-35.

705 Loubere, P., Gary, A., Lagoe, M., 1993. Benthic foraminiferal microhabitats and the generation of a  
706 fossil assemblage: Theory and preliminary data. *Marine Micropaleontology*, 20, 165-181.

707 Mackensen, A., Douglas, R.G., 1989. Down-core distribution of live and dead deep-water benthic  
708 foraminifera in box cores from the Weddell Sea and the California continental borderland. *Deep-Sea*  
709 *Research*, 36, 879-900.

710 McCorkle, D.C., Keigwin, L.D., Corliss, B.H., Emerson, S.R., 1990. The influence of microhabitats  
711 on the carbon isotopic composition of deep-sea benthic foraminifera. *Paleoceanography*, 5, 161-85.

712 Middelburg J.J., 2018. Reviews and syntheses: to the bottom of carbon processing at the seafloor  
713 *Biogeosciences*, 15, 413-427.

714 Middelburg, J.J., 2019. *Marine Carbon Biogeochemistry. A Primer for Earth System Scientists.*  
715 *SpringerBriefs in Earth System Sciences*. 188pp.

716 Mojtahid, M., Griveaud, C., Fontanier, C., Anschutz, P., Jorissen, F.J., 2010. Live benthic  
717 foraminiferal faunas along a bathymetrical transect (140-4800 m) in the Bay of Biscay (NE Atlantic).  
718 *Revue de Micropaléontologie*, 53, 139-162.

719 Moodley, L., Schaub, B.E.M., Van der Zwaan, G.J., Herman, P.M.J., 1998. Tolerance of benthic  
720 foraminifera (Protista: Sarcodina) to hydrogen sulphide. *Marine Ecology Progress Series*, 169, 77-86.

721 Mouret A., Anschutz P., Chaillou G., Hyacinthe C., Deborde J., Lecroart, P., Jorissen F.J., Deflandre  
722 B., Schmidt S., Jouanneau J.M., 2009. Benthic geochemistry of manganese in the Bay of Biscay. *Geo-*  
723 *Marine Letters*, 29, 133-149.

724 Mouret, A., Anschutz, P., Deflandre, B., Chaillou, G., Hyacinthe, C., Deborde, J., Etcheber, H.,  
725 Jouanneau, J.M., Grémare, A., Lecroart, P., 2010. Oxygen and organic carbon fluxes in sediments of  
726 the Bay of Biscay. *Deep-Sea Research I*, 528-540.

727 Mouret A., Anschutz P., Deflandre B., Deborde J., Canton M., Poirier D., Grémare A., Howa H.,  
728 2016. Spatial heterogeneity of benthic biogeochemistry in two contrasted marine environments  
729 (Arcachon bay and Bay of Biscay, SW France). *Estuarine, Coastal and Shelf Science* 179, 51-65.

730 Nomaki, H., Yamaoka, A., Shirayama, Y., Kitazato, H., 2007. Deep-sea benthic foraminiferal  
731 respiration rates measured under laboratory conditions. *J. Foram. Res.*, 37, 281-286.

732 Ogawa, N., Tauzin, P., 1973. Contribution à l'étude hydrologique et géochimique du Golfe de Cap-  
733 Breton. *Bulletin de l'Institut Géologique du Bassin d'Aquitaine*, Bordeaux, 14, 19-46.

734 Pina-Ochoa, E., Hogslund, S., Geslin, E., Cedhagen T., Revsbech, N.P., Nielsen, L.P., Schweizer, M.,  
735 Jorissen, F.J., Risgaard, S., Risgaard-Petersen, N., 2010. Widespread occurrence of nitrate storage and  
736 denitrification among Foraminifera and Gromiida. *PNAS* doi:10.1073/pnas.0908440107.

737 Rathburn, A.E., Corliss, B.H., 1994, The ecology of living (stained) deep-sea benthic foraminifera  
738 from the Sulu Sea: *Paleoceanography*, v. 9, p. 87-150.

739 Rathburn, A.E., Corliss, B.H., Tappa, K.D., Lohmann, K.C., 1996. Comparison of the ecology and  
740 stable isotopic compositions of living (stained) benthic foraminifera from the Sulu and South  
741 China Seas. *Deep-Sea Research* 43, 1617– 1646.

742 R Core Team, 2020. R: A Language and Environment for Statistical Computing. R Foundation for  
743 Statistical Computing, Vienna.

744 Richirt, J., Riedel, B., Mouret, A., Schweizer, M., Langlet, D., Seitaj, D., Meysman, F.J.R., Slomp,  
745 C.P., Jorissen, F.J., 2020. Foraminiferal community response to seasonal anoxia in Lake Grevelingen  
746 (the Netherlands). *Biogeosciences*, 17, 1415–1435, 2020.

747 Risgaard-Petersen N, Langezaal, A.M., Ingvardsen, S., Schmid, M.C., Jetten, M.S.M., Op den Camp,  
748 H.J.M., Derksen, J.W.M., Pina-Ochoa, E., Eriksson, S.P., Nielsen, L.P., Revsbech, N.P., Cedhagen,  
749 T., Van der Zwaan, G.J., 2006. Evidence for complete denitrification in a benthic foraminifer. *Nature*,  
750 443, 93–96. Ross, B.J., Hallock, P., 2016, Dormancy in the foraminifera: a review. *J. Foram. Res.*, 46,  
751 358-368.

752 Schmidt, S., Howa, H., Mouret, A., Lombard, F., Anschutz, P., Labeyrie, L., 2009. Particle fluxes and  
753 recent sediment accumulation on the Aquitanian margin of Bay of Biscay. *Continental Shelf Research*,  
754 29, 1044-1052.

755 Shirayama, Y., 1984. Vertical distribution of meiobenthos in the sediment profile in bathyal, abyssal  
756 and hadal deep sea systems of the western Pacific. *Oceanologica Acta*, 7, 123-29.

757 Soetaert, K., Meysman, F., 2012. Reactive transport in aquatic ecosystems: Rapid model prototyping  
758 in the open source software R *Environmental Modelling & Software*, 32, 49-60.

759 Soetaert K, Herman, P.M.J., Middelburg, J.J., 1996. A model of early diagenetic processes from the  
760 shelf to abyssal depths. *Geochim. Cosmochim. Acta*, 60, 1019-1040.

761 Soetaert K., Herman, P.M.J., 2009. A practical guide to ecological Modelling - using R as a simulation  
762 platform. Springer, 377 pp.

763 Straub, K.L., Benz, M., Schink, B., Widdel, F., 1996. Anaerobic, Nitrate-Dependent Microbial  
764 Oxidation of Ferrous Iron. *Applied and Environmental Microbiology*, 62, 1458-1460.

765 Van der Zwaan, G. J., Duijnste I. A. P., Den Dulk M., Ernst S. R., Jannink N. T., Kouwenhoven T. J.,  
766 1999. Benthic foraminifers: proxies or problems? A review of paleocological concepts. *Earth Sci. Rev.*  
767 46, 213–236.



805 **1. Introduction**

806 Since the pioneering work of Corliss and his colleagues in the 1980's (Corliss, 1985; Corliss & Chen  
807 1988; Corliss and Emerson, 1990) – which has been fully confirmed by a number of subsequent  
808 studies (i.e., Gooday, 1986; Mackensen and Douglas, 1989; McCorkle et al. 1990; Rathburn & Corliss,  
809 1994; Jorissen et al., 1998) – we know that in open marine settings, there is a vertical succession of  
810 benthic foraminiferal species in the surface sediment. This species succession, which appears to be  
811 closely related with the well-known succession of redox layers in the surface sediment (e.g., Froelich  
812 et al., 1979, Canfield et al., 1993) may be expanded over several centimetres (up to ~10 cm at most)  
813 or be compressed in the first few millimetres of the sediment. Despite of this vertical variability, the  
814 succession of foraminiferal species is always the same (Jorissen, 1999a). Consequently, foraminiferal  
815 species may be considered as shallow, intermediate or deep infaunal, not so much on the basis of the  
816 exact depth at which they are found in the sediment column, which can vary considerably, but rather  
817 on their relative position in the vertical species succession (Jorissen et al., 2007).

818 Following earlier suggestions of Shirayama (1984), Corliss and Emerson (1990) and Loubere et al.  
819 (1993), Jorissen et al. (1995) proposed the so-called TROX-model, which hypothesized that the  
820 vertical penetration depth of foraminiferal species into the sediment is determined by food  
821 availability in oligotrophic ecosystems, but would be limited by redox conditions (especially by pore  
822 water oxygen concentration and by the presence of toxic dissolved sulphides) in eutrophic settings.  
823 Different requirements with respect to these limiting factors would then explain the specific  
824 microhabitats of individual species. Indirectly, the TROX model also explains biodiversity trends,  
825 which are strongly affected by the availability or not of ecological niches deeper in the sediment. This  
826 conceptual model has since been confirmed by a large number of observational studies, and it has  
827 also been proposed to explain macrofaunal distribution patterns (Carney, 2005).

828 Since 1995, several authors have tried to further elaborate upon the TROX model, by integrating  
829 bioturbation (Van der Zwaan et al., 1999), or by coupling the foraminiferal distribution with several  
830 redox species (Koho et al., 2015), and not only with oxygen, as in the original model. In the 25 years  
831 since the publication of the TROX model, we have also learned a lot about benthic foraminiferal  
832 ecology. After the ground-breaking publications of Risgaard-Petersen et al. (2006), Høglund et al.  
833 (2008), Pina-Ochoa et al. (2010) and Bernhard et al. (2012), we know that many species are capable  
834 of storing nitrate in their protoplasm, and at least some of these species are capable of respiring  
835 nitrate when confronted with anoxia. For other taxa, a capability to sequester chloroplasts from  
836 consumed diatoms has been shown (e.g., Lee and Anderson, 1991; Bernhard and Bowser, 1999). The  
837 foraminifera are able to keep these intracellular chloroplasts active for several weeks, showing  
838 another foraminiferal strategy for survival under strongly adverse conditions (Jauffrais et al., 2016).  
839 And finally, a last group of species may survive adverse conditions by entering into a state of  
840 dormancy, with a strongly diminished metabolic rate (Bernhard and Alve, 1997; Ross and Hallock,  
841 2016).

842 The presence of an alternative metabolic pathway, in facultatively anaerobic taxa, as well as the  
843 other metabolic adaptations, explains why most benthic foraminiferal species are tolerant to strong  
844 hypoxia (at least down to ~0.5 ml/l, or 22 µmol/l; Jorissen et al., 2007). This also explains how  
845 foraminifera can survive, and for some species at least, remain active in anoxic conditions. In this  
846 context, several observational studies have shown foraminiferal survival after exposure to anoxia  
847 together with free sulphides (e.g., Langlet et al., 2013; 2014, Richirt et al., 2020), a combination  
848 which until recently was generally considered lethal (Moodley et al., 1998). The ultimate  
849 disappearance of benthic foraminifera during cases of long-term anoxia, as is for instance observed  
850 in Mediterranean sapropels (e.g., Jorissen, 1999b), seems therefore not to be the consequence of

851 strongly increased mortality, but rather of an inhibition of reproduction under strongly adverse  
852 conditions (Richirt et al., 2020).

853 These recent advances suggest that oxygen may not be the foremost environmental parameter  
854 explaining foraminiferal ecology, as was often thought in the past (e.g., Bernhard, 1886; Alve and  
855 Bernhard, 1995), and was more or less hypothesized in the TROX model. Instead, it appears that it is  
856 rather the quantity, and especially the quality of the food particles, that are the predominant  
857 parameters. However, the quality of the organic matter ( $C_{org}$ ) flux will also affect the biological  
858 oxygen demand, and thereby the bottom water and sediment redox conditions, so that the  
859 combination of the organic matter flux and oxygen content forms an inextricable complex.

860 Despite the determinant role of the organic matter flux, oxygen will still be a principal controlling  
861 factor when values are close to (or below) the tolerance levels of many species and/or higher  
862 taxonomical categories. Although alternative metabolic pathways for organic matter decomposition  
863 can be utilized under suboxic and anoxic conditions, they are energetically much less favourable,  
864 with the exception of denitrification (Froelich et al., 1979; Middelburg, 2019).

865 Furthermore, we have indications that the presence of free sulphides is not directly lethal (Bernhard  
866 et al., 1993; Langlet et al., 2014), but that long-term exposure leads to a decrease of foraminiferal  
867 population densities (Moodley et al., 1998; Richirt et al., 2020). It has been suggested that this would  
868 be due to a decrease of metabolic rate, and a loss of vital functions, such as growth, and especially  
869 reproduction (Moodley et al., 1998; Richirt et al., 2020). Long-term exposure to dissolved sulphides  
870 should therefore ultimately lead to the disappearance of foraminifera.

871

872 Summarising, even if our ideas about the specific role of some environmental factors, such as oxygen  
873 availability, have become more nuanced, the importance of redox conditions within the foraminiferal  
874 microhabitat remains paramount, and consequently, the conceptual TROX model (Jorissen et al.,  
875 1995) still provides an excellent tool to understand foraminiferal distribution patterns.

876

877 In this paper, we present a first attempt to translate the conceptual TROX-model into a numerical  
878 model, combining sediment early diagenesis (the combination of biological, chemical, and physical  
879 processes which change the quantity and composition of the organic matter before they become  
880 consolidated; Henrichs, 1992) and foraminiferal ecology.

881 The aim of such a model is that it will allow us to test hypotheses concerning foraminiferal ecology.  
882 We will define theoretical species, with distinct characteristics, that each represent a group of real  
883 species with a similar microhabitat. We will then see how these theoretical species behave (are  
884 distributed) in the vertical succession of redox zones reproduced by the model, and compare the  
885 model results with observational data. If the model is capable of successfully reconstructing the field  
886 observations, this means that the underlying hypotheses concerning the foraminiferal ecology may  
887 be realistic. If this is not possible, the way the foraminiferal species are defined is probably incorrect.

888 Ultimately, the aim is to use this model as a tool to test paleoceanographical scenarios and to  
889 reconstruct environmental parameters from foraminiferal successions in fossil records.

890 For the construction of the model, we profit from an extremely favourable context. First, early  
891 diagenetic models have become widely available. We decided to use the OMEXDIA model of Soetaert  
892 et al. (1996), which is well established, very well documented (Soetaert and Hermann, 2009) and  
893 freely available on the Comprehensive R Archive Network (<https://cran.r-project.org>). The OMEXDIA  
894 model will be coupled to a new foraminiferal model developed in the present study. Next, we employ  
895 a very large mixed database of sediment geochemistry (Anschutz et al., 1999, 2005; Hyacinthe et al.,

896 2001, Chaillou et al., 2002, 2003, 2006; Mouret et al., 2009, 2010; Schmidt et al., 2009) and  
897 foraminiferal distribution (Fontanier et al., 2002, 2003, 2005, 2006a; Langezaal et al., 2006; Mojtahid  
898 et al., 2010) for the Bay of Biscay. We decided to use the data collected between 1997 and 2001,  
899 when a bathymetrical transect from 150 to 2000 m water depth was sampled 10 times. This data set  
900 gives ample insight into seasonal and interannual variability of sediment geochemistry and  
901 foraminiferal communities. We will use this very large dataset to calibrate the model, and to test it in  
902 two different ecological settings.

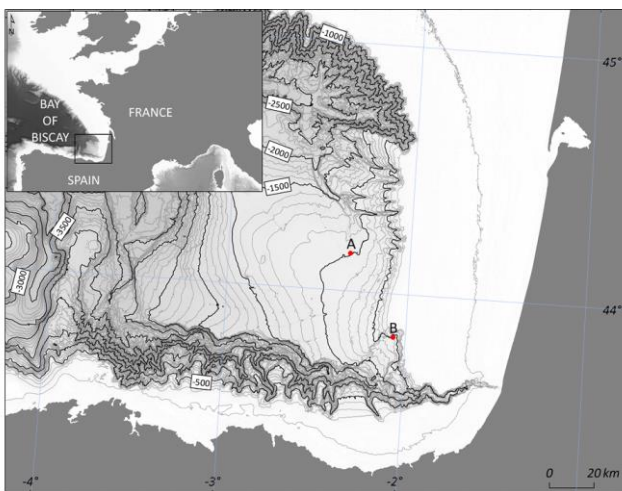
903 This paper presents the first results of this exercise, in which the numerical model is developed, and  
904 is manually tested and tuned at two sampling stations, at 1000 and 550 m depth in the Bay of Biscay.  
905 In the process of developing the model, we sequentially tested a range of hypotheses regarding the  
906 benthic environment and its link to foraminiferal ecology. To illustrate the value of quantitative  
907 models for such hypothesis testing, we present this study in a manner that emphasizes the  
908 sequential steps in model development and calibration, highlighting the lessons learned along the  
909 way.

910 **2. Model characteristics**

911 When we set out to develop the coupled early diagenesis – benthic foraminiferal ecology model  
912 presented here, we chose to implement the model in the software R (R Core Team, 2020). R is widely  
913 used for scientific programming, and is freely available (<https://www.r-project.org>). We decided to  
914 use the early diagenetic model (1D) of Soetaert, which has been described in a number of  
915 publications (Soetaert et al., 1996; Soetaert & Herman, 2009), and is freely available online in the R-  
916 package 'ReacTran' (Soetaert and Meysman, 2012; [http://](http://www.rforscience.com/modelling/omexdia/)  
917 [www.rforscience.com/modelling/omexdia/](http://www.rforscience.com/modelling/omexdia/)).

918 The next step was to introduce theoretical species of benthic foraminifera, with different ecological  
919 characteristics (each theoretical species represents a group of real species), into this 1D geochemical  
920 environment. At a first stage, we investigated the possibility of constructing a quantitative biological  
921 model, including the most important life functions (e.g., growth, reproduction, mortality, etc.) of the  
922 different species. However, it soon turned out that this approach was severely hampered by a lack of  
923 observational data for most of these parameters. For this reason, we decided to change our strategy,  
924 and instead developed a “transformation model”, in which a fraction of the available resources was  
925 allocated to different members of the benthic foraminiferal community. More precisely, we assigned  
926 different proportions of the various types of organic matter ( $C_{org}$ ), more or less reactive, to the  
927 foraminiferal species introduced into the model.

928 We then tested the model on our extensive geochemical and foraminiferal dataset from the Bay of  
929 Biscay. After constructing the essential components of the model, we started to tune the model  
930 using the data of stations A and B, at 1000 and 550 m depth, respectively. We first optimized the fit  
931 between the geochemical data and the model results. Next, we tested various hypothesis concerning  
932 the ecological requirements of the benthic foraminifera, in order to obtain a maximum resemblance  
933 between observational data and model output.



934  
935 Fig. 1. Map of the bay of Biscay, with sampling stations A (1000 m) and B (550 m).  
936

937 **3. The Bay of Biscay data set**

938 Bay of Biscay Stations A, at 1000 m water depth, and B, at 550 m depth, were visited 15 times  
939 between October 1997 and February 2011. The surficial sediment was sampled with an interface  
940 multi-corer, which allowed sampling the upper few decimetres of the sediment, the overlying  
941 bottom water, and the undisturbed sediment-water interface, in a 10 cm diameter Plexiglas tube. At  
942 both stations, very similar profiles of redox reactive compounds were measured in the numerous  
943 short cores collected over the 14 year interval (Mouret et al., 2016). Only small differences were  
944 noticed at the sediment surface, which were attributed to seasonality, bioturbation and/or spatial  
945 patchiness. For the present study we decided to concentrate on the period between October 1997  
946 and September 2001, when these stations were sampled 10 times, so that the seasonal and  
947 interannual variability of the geochemical composition of bottom and pore waters, as well as of the  
948 foraminiferal community, is particularly well constrained. The pore water geochemistry of these  
949 station has been described in detail by Hyacinthe et al. (2001), Anschutz et al. (2005), Mouret et al.  
950 (2009, 2010) and Charbonnier et al. (2019). Schmidt et al. (2009) concentrated on the particle fluxes  
951 and sediment accumulation rate. The foraminiferal community at the two stations was described by  
952 Fontanier et al. (2002; 2003; 2006a) and Mojtahid et al. (2010). Important seasonal and interannual  
953 variability was observed for the foraminiferal density and species composition. It appears that  
954 foraminiferal densities increased to an order of magnitude after major spring and autumn  
955 phytoplankton blooms, which favoured a limited number of opportunistic benthic foraminiferal taxa  
956 (Fontanier et al., 2003; 2006a).

957 In view of the observed stability of the succession of sediment redox zones (Mouret et al., 2009), we  
958 decided to use an averaged geochemical data set to calibrate our diagenetic model. To this purpose,  
959 for every geochemical model parameter, the observations for all available sampling campaigns (their  
960 number varied for different parameters) were averaged, so that a single value was obtained for all  
961 depth levels down to 10 cm depth in the sediment. For this first modelling study, foraminiferal data  
962 were averaged as well, for the 10 successive sampling campaigns.

#### 963 4. Early Diagenesis Model Parameters

964 The first portion of our model utilizes OMEXDIA, a reactive transport model for evaluating  
965 sedimentary diagenesis (Soetaert et al., 1996), which was run to steady state. It includes multiple  
966 organic matter remineralization pathways, incorporates key diagenetic chemical reactions, and  
967 allows for depth-dependent bioturbation/biodiffusion and porosity. In the present study, many of  
968 the key parameters of the model are constrained by observations derived from prior studies of  
969 stations A and B. Using the dataset of stations A and B, the model was manually tuned to provide  
970 initial constraints for the complete model, discussed later. The values of the main parameters used  
971 as starting point for the early diagenesis part of the model were the following:

- 972 • The organic carbon flux ( $C_{org}$ ) to the sea floor: for the 1000 m deep station A, Mouret et al.  
973 (2010) estimated a total  $C_{org}$  flux of  $16.5 \text{ gC m}^{-2} \text{ yr}^{-1}$ , consisting of 76% labile particulate  
974 organic carbon (POC), 9% slowly decaying POC, and 15% inert POC. At the 550 m deep  
975 station B, Mouret et al. (2010) estimated a total  $C_{org}$  flux of  $28.2 \text{ gC m}^{-2} \text{ yr}^{-1}$ , with 53.6% labile  
976 POC, 20.4% slowly degrading POC and 26.0% inert POC. These values were used as the basis  
977 for our tuning exercise. The most labile fraction was deduced from modelled dissolved  
978 oxygen consumption at the sediment surface. Other fractions were deduced from  $C_{org}$   
979 concentrations and mass accumulation rates.
- 980 • Bottom water temperature was always  $9.5^\circ\text{C}$  at station A, and  $11.0^\circ\text{C}$  at station B, without  
981 any seasonal variability (Ogawa et al., 1973; Durrieu de Madron et al., 1999 and Fontanier et  
982 al., 2006b).
- 983 • Bottom water oxygenation varied between  $189$  and  $201 \mu\text{mol l}^{-1}$  at station A and between  
984  $205$  and  $221 \mu\text{mol l}^{-1}$  at station B (Mouret et al., 2010; Anschutz and Chaillou; 2009).
- 985 • At both stations A and B, the sediment was a silty clay, with a mean grain size of  $5\text{--}6 \mu\text{m}$  at  
986 station A and  $10\text{--}15 \mu\text{m}$  at station B (Charbonnier et al., 2019). The sediment contained about  
987  $30\%$   $\text{CaCO}_3$  at station A, versus  $10\text{--}15\%$  at station B. At both stations, sediment porosity  
988 decreased quickly in the first millimeters of the sediment, from  $0.85$  at the sediment-water  
989 interface to about  $0.8$  at  $1 \text{ cm}$  depth. Deeper down, porosity continued to decrease, until  
990 values between  $0.65$  and  $0.7$  were observed at  $10 \text{ cm}$  depth at stations A and B, respectively.
- 991 • The oxygen penetration depth into the sediment varied from  $1.6$  to  $2.2 \text{ cm}$  at station A, and  
992 from  $1.1$  to  $1.9 \text{ cm}$  at station B (Fontanier et al., 2003; 2006a; Mouret et al., 2010).
- 993 • At station A, nitrate in the bottom waters, sampled in the supernatant water of the sediment  
994 cores, varied from  $8.6$  to  $21.1 \mu\text{mol l}^{-1}$ , with a mean value of  $14.3 \mu\text{mol l}^{-1}$ . At station B,  
995 nitrate varied from  $11.5$  to  $15.7 \mu\text{mol l}^{-1}$ , with a mean value of  $14.1 \mu\text{mol l}^{-1}$ . These values are  
996 very close to those measured on water column samples taken with Niskin bottles (Anschutz  
997 and Chaillou, 2009). Maximum nitrate concentrations were generally observed in the top  $2$   
998  $\text{cm}$  of the sediment, with values of  $24$  to  $33 \mu\text{mol l}^{-1}$  at station A, and  $19$  to  $23 \mu\text{mol l}^{-1}$  at  
999 station B. Deeper down, nitrate concentrations strongly decreased, with values below  $23$   
1000  $\mu\text{mol l}^{-1}$  reached between  $4$  and  $5 \text{ cm}$  at station A and around  $2 \text{ cm}$  at station B. Ammonia  
1001 always showed a strong downward increase from values around zero at the surface to mean  
1002 values of  $30.7 \mu\text{mol l}^{-1}$  (station A) and  $61.1 \mu\text{mol l}^{-1}$  (station B) at  $10 \text{ cm}$  depth.
- 1003 • Among the reduced components, dissolved  $\text{Mn}^{2+}$  and  $\text{Fe}^{2+}$  were only determined for part of  
1004 the  $10$  sampling campaigns (Mouret et al., 2009), whereas no data for  $\text{S(-II)}$  were available.  
1005 The sulphate concentration was constant with depth and equal to the  $\text{SO}_4^{2-}$  concentration in  
1006 seawater. No sulphide smell was evident during core processing, but a few black patches  
1007 were observed near the base of the cores, suggesting  $\text{H}_2\text{S}$  production in deeper sediment  
1008 layers (Chaillou et al. 2003). Since the  $\text{H}_2\text{S}$  concentration was not measured, the model  
1009 output for ODU (oxygen demand units, i.e. the amount of oxygen necessary to reoxidize

1010 reduced counterparts from anaerobic mineralization), which regroups all reduced  
1011 components, was always higher than the observations, which include only measured  
1012 dissolved Mn and Fe.

- 1013 • At station A, the maximum sediment accumulation rate was estimated on the basis of <sup>210</sup>Pb  
1014 profiles at 0.068 cm/year (36 mg cm<sup>-2</sup> yr<sup>-1</sup>) by Chaillou et al. (2002), at 0.05 to 0.06 cm/year  
1015 by Schmidt et al. (2009), whereas Mouret et al., 2009 obtained a value of 0.062 cm/year  
1016 based on steady state manganese diagenesis. For station B, Chaillou et al. (2002) obtained a  
1017 maximum sedimentation rate of 0.15 cm/year (79.5 mg cm<sup>-2</sup> yr<sup>-1</sup>), compared to values of 0.12  
1018 and 0.22 cm/year by Schmidt et al. (2009), and 0.12 cm/year based on steady state  
1019 manganese diagenesis (Mouret et al., 2009).
- 1020 • Mouret et al. (2009) obtained a large variety in biodiffusion coefficients, using <sup>234</sup>Th profiles,  
1021 for sediment cores sampled during four different campaigns, with values varying between  
1022 0.12 and 6.7 cm<sup>2</sup>/year at station A, and between 0.4 and 14.8 cm<sup>2</sup>/year at station B. They  
1023 estimated a mixed layer depth of about 1cm at both stations, slightly less than the depth of  
1024 the oxic layer.

1025 Despite the lack of observational data for some parameters (such as sulphur) in some of the  
1026 cores, and the large variability observed for biodiffusion coefficients, the Bay of Biscay dataset  
1027 for these two stations is remarkable by its near completeness for 10 successive sampling  
1028 campaigns. It therefore forms an ideal dataset to develop and test our early diagenetic model.  
1029 The main parameter that we used to tune the model was the C<sub>org</sub> flux to the sea floor, or more  
1030 precisely the proportions and reactivity constants of the various types of organic matter. A  
1031 secondary main tuning parameter was the rate of pyrite formation in the sediment; this process  
1032 withdraws reduced components from the pore water.

1033

1034 **5. Initial tuning of the preliminary (3G) early diagenetic model, using the station A data set**

1035 Before introducing theoretical foraminiferal species into the model, our first objective was to tune  
1036 the early diagenetic model to obtain an optimal fit between the averaged observed data and the  
1037 model output. For this initial tuning exercise, we used the dataset for station A. Fig. 2 gives an  
1038 example of an early result that employed three types of organic matter (3G).

1039

1040

1041

1042

1043

1044

1045

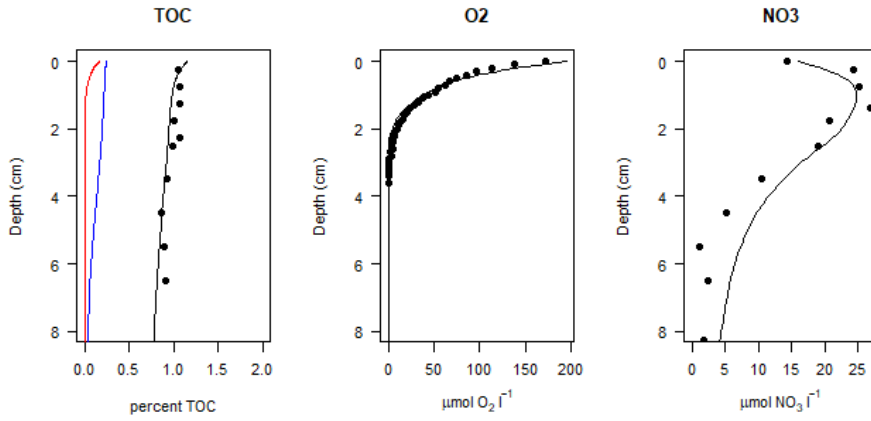
1046

1047

1048

1049

1050



1051

1052

1053

1054

1055

1056

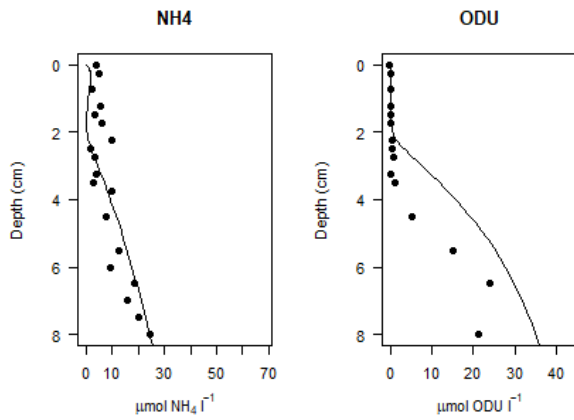
1057

1058

1059

1060

1061



1062 Fig. 2. Station A - Model output for early diagenetic parameters (lines) of a preliminary version of the 4GFOR  
 1063 model, with only three types of organic matter (percent TOC = particulate  $C_{org}$  in weight % of dry sediment; red:  
 1064 fast degrading, blue: intermediate, black: total organic carbon (= fast degrading + intermediate + fossil),  
 1065 compared to observational data from Station A (dots).

1066 It can be seen that the model results for  $C_{org}$ , oxygen and ammonia are very close to the observed  
 1067 data. However, although the modelled ODU curve has the right form, the absolute values are much  
 1068 higher than the observed ones. As explained in the previous section, this is likely due to the fact that  
 1069 only Fe and Mn were measured, and not S, a third major component contributing to ODU. As we do  
 1070 not intend to use ODU as a limiting factor for the foraminiferal species, we do not consider this very  
 1071 important. The main problem with this preliminary model is the nitrate curve, which in deeper  
 1072 sediment layers showed values that are too high compared to the observed ones. This is important,  
 1073 because we intend to use a minimum  $NO_3^-$  concentration as a switch for nitrate-respiring  
 1074 foraminifera in the subsequent foraminiferal component of the model. All our attempts to improve  
 1075 the fit for nitrate systematically resulted in an upward movement of the oxygen profile, which is even  
 1076 more problematic, because we intend to use oxygen concentration as a switch for obligate aerobic  
 1077 foraminiferal species. In the final version of the model we resolved this problem by adding an

1078 additional diagenetic pathway, ferrous iron nitrification. This reaction, the anaerobic oxidation of  $\text{Fe}^{2+}$   
1079 by nitrates (e.g., Straub et al., 1996; Kappler et al., 2021), appears to be an important process at our  
1080 sites in the Bay of Biscay (Hyacinthe et al., 2001), and was hitherto not included in the OMEXDIA  
1081 model. This early diagenetic pathway consumes nitrate at the lower part of its range, and diminishes  
1082 ODU. After adding this reaction, to the early diagenetic part of the model, we arrived at excellent fits  
1083 for all parameters except ammonia, which was overestimated (Fig. 5). Since ammonia has no impact  
1084 on the faunal distribution, this was considered less important.

## 1085 6. Defining the foraminiferal species

1086 As explained before, we decided not to include a fully biological model for the foraminiferal species,  
1087 but rather a transformation model. This transformation model has two basic characteristics. First,  
1088 foraminiferal activity is limited by critical environmental factors, such as oxygen and nitrate content.  
1089 Beyond the critical threshold values, specified foraminifera are no longer given access to the  
1090 available resources. Next, when these limiting factors are within the tolerance limits of the organism,  
1091 a specific proportion of each type of  $C_{\text{org}}$  is attributed to each of the species. In the way we defined  
1092 them, species living close to the sediment surface use a large proportion of reactive  $C_{\text{org}}$ , whereas  
1093 species living deeper in the sediment use a larger proportion of slowly degrading  $C_{\text{org}}$ . This  
1094 interspecific difference is based on two assumptions: 1) that infaunal foraminiferal taxa are better  
1095 capable than surface dwellers to feed on organic matter of a lower quality, and 2) that sediment  
1096 surface dwellers are more competitive than infaunal taxa when the uptake of high quality (highly  
1097 reactive)  $C_{\text{org}}$  is concerned.

1098 The allocation of different proportions of various qualities of organic carbon to different species is  
1099 reminiscent of the BFAR-concept of Herguera and Berger (1991). In fact, Herguera and Berger  
1100 assumed that for every mg of  $C_{\text{org}}$  arriving at the sea floor, roughly one foraminiferal shell  $> 150 \mu\text{m}$   
1101 would be preserved in the sediment record.

1102 In our first attempts to model the foraminiferal distribution in the sediment (for station A), we used a  
1103 3G diagenetic model, with fast, slowly degrading, and inert  $C_{\text{org}}$ ; a very good fit between model  
1104 output and observed data was obtained with decay rates  $r_{\text{fast}} = 0.01/\text{day}$ ,  $r_{\text{slow}} = 0.00005/\text{day}$  and  $r_{\text{fossil}} = 0$ . In these first runs (Fig. 3), we introduced only 2 foraminiferal species:

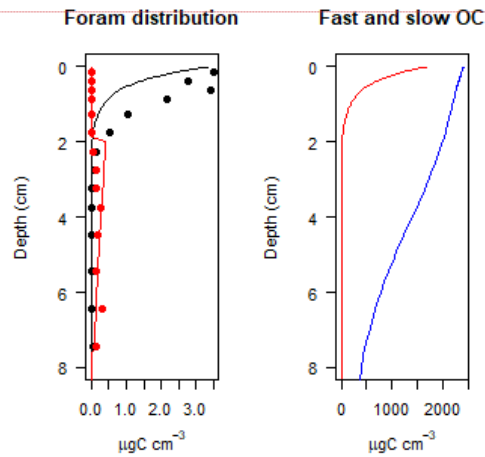
1106 1) an epifaunal/shallow infaunal species, which was dependant on the presence of oxygen, at least at  
1107 very low concentrations ( $\text{O}_2 > 2.5 \mu\text{mol l}^{-1}$ ). We defined this species group so that it exclusively feeds  
1108 on fast decaying  $C_{\text{org}}$ .

1109 2) a deep infaunal species, which we inhibited by oxygen ( $\text{O}_2 \leq 2.5 \mu\text{mol l}^{-1}$ ), but which was dependent  
1110 on the presence of nitrate ( $\text{NO}_3 > 2.5 \mu\text{mol l}^{-1}$ ), and given access to both fast and slowly degrading  
1111  $C_{\text{org}}$ .

1112 In order to compare the model outcome (in  $\text{mgC cm}^{-3}$ ) with the observational data (observed number  
1113 of tests  $> 150 \mu\text{m}$ ), we assumed that a single foraminiferal individual ( $> 150 \mu\text{m}$ ) of the  
1114 epifaunal/shallow infaunal species would contain  $0.625 \mu\text{g } C_{\text{org}}$ , whereas a deep infaunal individual ( $>$   
1115  $150 \mu\text{m}$ ) would on average contain  $3.6 \mu\text{g } C_{\text{org}}$ . These foraminiferal  $C_{\text{org}}$  contents are based on the  
1116 relationship between biovolume and protein content observed by Movellan et al. (2012), assuming  
1117 an average size of  $250 \mu\text{m}$  for epifaunal/shallow infaunal taxa (considered as semi-spheres,  
1118 representative of most epifaunal and trochospiral taxa) and of  $450 \mu\text{m}$  for deep infaunal taxa  
1119 (considered as a cylinder, such as *Globobulimina* spp.).

1120

1121  
1122  
1123  
1124  
1125  
1126  
1127  
1128  
1129  
1130  
1131



Commenté [f1]: Change slow in intermediate ?!

1132 Fig. 3. First results of the coupled 3G early diagenesis (using two types of reactive organic matter) -  
1133 foraminiferal model. Left panel: epifaunal/shallow infaunal taxa (black) and deep infaunal taxa (red). Right  
1134 panel: fast degrading  $C_{org}$  (red) and intermediate degrading  $C_{org}$  (blue) Dots = observed data for station A (1000  
1135 m depth); lines = model output. Epifaunal/shallow infaunal taxa (black curve) only have access to fast decaying  
1136 organic matter.

1137

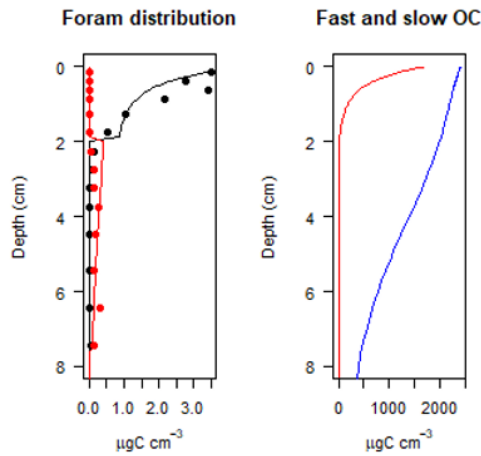
### 1138 7. Further developing the (3G) early diagenesis – perfecting the foraminiferal model for 1139 station A

1140 The first results of the coupled early diagenesis-foraminifera model for the 1000 m deep station A  
1141 (Fig. 3) were encouraging. To arrive at this fit, we attributed 0.2% of fast decaying  $C_{org}$  to  
1142 epifaunal/shallow infauna (when  $O_2 > 2.5 \mu\text{mol l}^{-1}$ , left panel, black curve), and 0.1% of fast decaying  
1143  $C_{org}$  and 0.002% of slowly decaying  $C_{org}$  to deep infauna (when  $O_2 \leq 2.5 \mu\text{mol l}^{-1}$  and  $NO_3 > 2.5 \mu\text{mol l}^{-1}$ , left panel, red curve).

1145 These values, which were selected to obtain a reasonable fit, are in reality thought to reflect the  
1146 capacity of these species to feed on various types of  $C_{org}$ , and their competitive success compared to  
1147 other (foraminiferal as well as non foraminiferal) organisms feeding on the same resources. For  
1148 comparison, for continental shelf (37-60 m depth) and upper slope (450 m depth) environments with  
1149 well oxygenated bottom waters, Geslin et al. (2011) estimated the total foraminiferal contribution to  
1150 dissolved oxygen utilisation at 0.5 to 2.5%.

1151 However, although the obtained result (Fig. 3) was encouraging, it was not yet fully acceptable.  
1152 There were in fact three major problems. The first problem was that the epifaunal/shallow infaunal  
1153 taxon did not penetrate deep enough into the sediment; their strong decline in the first cm of the  
1154 sediment is the direct consequence of the similar decline of the fast degrading  $C_{org}$  (red curve in the  
1155 right panel of fig. 3). In our opinion, the model results clearly show, that our initial hypothesis, that  
1156 epifaunal/shallow infaunal taxa exclusively feed on fast degrading  $C_{org}$ , is not supported. We solved

1157 this problem by  
1158 small fraction (0.004%)  
1159 degrading  $C_{org}$  to  
1160 infaunal species (Fig.



attributing also a  
of slowly  
epifaunal/shallow  
4).

1161  
1162  
1163  
1164  
1165  
1166  
1167  
1168  
1169  
1170

1171 Fig. 4. First results of the coupled (3G) early diagenesis (using three types of organic matter) - foraminiferal  
1172 model for station A (1000 m depth). Left panel: epifaunal/shallow infaunal taxa (black) and deep infaunal taxa  
1173 (red). Right panel: fast degrading  $C_{org}$  (red) and intermediate degrading  $C_{org}$  (blue). Dots = observed data; lines =  
1174 model output. Epifaunal/shallow infaunal taxa now have also access to a small part of slowly degrading  $C_{org}$ .

1175 The second problem was the fact that in reality, there are more than two groups of foraminiferal  
1176 species. There are not only deep infaunal species (such as *Globobulimina* spp.), but also intermediate  
1177 infaunal species, such as *Melonis barleeanus*, which always attain the highest density at the depth  
1178 where nitrate concentration is maximal (e.g., Jorissen et al., 1998). In addition, the group of  
1179 epifauna/shallow infauna seems to be more complex, with some taxa always living close to the  
1180 sediment-water interface, and others living slightly deeper in the oxygenated part of the surficial  
1181 sediment. The first group is dominated by trochospiral genera (*Cibicidoides*, *Gyroidina*, *Hoeglundina*,  
1182 *Oridorsalis*, etc.), whereas the second group is rather dominated by triserial and biserial genera  
1183 (*Bolivina*, *Bulimina*, *Trifarina*, *Uvigerina*, etc.).

1184 In order to take into account this complexity, we decided to expand our model to four theoretical  
1185 foraminiferal taxa, each of which is supposed to represent a group of real species with similar  
1186 microhabitat characteristics. Since we think that the name “epifauna” should be reserved for taxa  
1187 living on elevated substrates above the sediment, we will use the terms “shallow infauna A” (SIA),  
1188 “shallow infauna B” (SIB), “intermediate infauna” (II) and “deep infauna” (DI) for our four theoretical  
1189 species (groups) living at increasingly greater depth in the sediment.

1190 In order to model the vertical distribution of these four theoretical species, it soon turned out that a  
1191 rough subdivision of the organic carbon resources into three types (fast degrading, slowly degrading,  
1192 fossil) was insufficient. For this reason, we shifted to the final 4G model, with three types of reactive  
1193  $C_{org}$ : fast, intermediate and slowly degrading, and finally inert  $C_{org}$ .

1194 The final problem was that in the first versions of the model (Figs. 3, 4), we inhibited the activity of  
1195 the deep infaunal species with oxygen. However, Nomaki et al. (2007) observed oxic respiration for  
1196 the deep infaunal taxa *Globobulimina affinis* and *Chilostomella ovoidea*. Consequently, in most

1197 studies, deep infaunal taxa are considered as facultative anaerobes, which will only shift to an  
1198 anaerobic metabolism (using nitrate) when no oxygen is available.

1199 We solved this problem by replacing the inhibition with an additional scaling factor. In fact, we  
1200 defined the intermediate and deep infaunal categories in such a way that the amount of fast and  
1201 intermediate degrading  $C_{org}$  allocated to them decreases exponentially towards higher oxygen  
1202 concentration. In biological terms, this means that these taxa become rapidly less competitive  
1203 (compared to shallow infaunal groups A and B) when oxygen concentrations increase. In our opinion,  
1204 this is a very realistic way to define these species for the sake of our quantitative model.

1205 **8. Tuning the final 4GFOR Model for stations A (1000 m) and B (550 m).**

1206 Concerning the final tuning of the early diagenesis part of the 4GFOR model, an optimal fit between  
1207 model output and observations was obtained by using a total  $C_{org}$  flux of 16.0 and 25.0  $\text{gC m}^{-2} \text{yr}^{-1}$  at  
1208 stations A and B, respectively (table 1). These values are very close to the values of 16.5 and 28.2  $\text{gC}$   
1209  $\text{m}^{-2} \text{yr}^{-1}$  given by Mouret et al., 2010).

1210

---

---

---

Parameter	Description	Station A	Station B	Unit	Source
maxdep	Maximum depth for modeled sediment	24	24	cm	I
pO	Porosity in surface sediment	83.3	88.5	%	I
pinf	Porosity at maximum modeled depth	64.2	69.7	%	I
pco	Coefficient of decrease for porosity	4.47	2.76		I
sedr	Sedimentation rate	0.055	0.15	cm/year	L <sup>6</sup>
Db	Bioturbation rate	0.75	1.25	cm/year	L <sup>3</sup>
mixl	Mixed layer depth	1.0	1.0	cm	L <sup>3</sup>
fluxm	Total Corg flux at sediment water interface	16.0	25.0	g m <sup>-2</sup> y <sup>-1</sup>	L <sup>3</sup> ; C
TCorginf	%Corg at infinite depth	0.79	0.83	%	L <sup>3</sup>
rfast	1st order rate constant for fast degrading Corg	0.026	0.015	day <sup>-1</sup>	C
rint	1st order rate constant for intermediately degrading Corg	0.001	0.0005	day <sup>-1</sup>	C
rslow	1st order rate constant for slowly degrading Corg	0.00003	0.000025	day <sup>-1</sup>	C
pfast	fraction of fast degrading Corg in total Corg flux	58.41	34.0	%	C
pint	fraction of intermediate degrading Corg in total Corg flux	20.0	21.5	%	C
pslow	fraction of slow degrading Corg in total Corg flux	6.26	18.5	%	C
NCrFdat	NC ratio fast decay det	0.16	0.16	molN/molC	L <sup>5</sup> ; C
NCridat	NC ratio intermediate decay det	0.2	0.2	molN/molC	C
NCrSdat	NC ratio slow decay det	0.13	0.13	molN/molC	L <sup>5</sup>
Pdepo	Fraction of ODU production deposited as solid	0.44	0.44	% day <sup>-1</sup>	L <sup>5</sup>
Temp	Bottom water temperature	9.5	11	°C	L <sup>2,4</sup>
bwO2	Oxygen concentration in bottom water	196.5	213.4	mmol m-3	L <sup>3</sup> ; I
bwNO3	Nitrate concentration in bottom water	16	14	mmol m-3	L <sup>1</sup> ; I
bwNH3	Ammonia concentration in bottom water	0	0.6	mmol m-3	L <sup>1</sup> ; I
NH3bot	Ammonia conc at bottom modeled sediment column	68.29	200	mmol m-3	I
ksO2oxic	Half-saturation O2 in oxic mineralisation	30	30	mmol m-3	L <sup>5</sup>
ksNO3denit	Half-saturation NO3 in denitrif	15	15	mmol m-3	L <sup>5</sup>
kinO2denit	Half-saturation O2 inhib denitrif	0.5	0.5	mmol m-3	L <sup>5</sup>
kinNO3anox	Half-saturation NO3 inhib anoxic min	1	1	mmol m-3	L <sup>5</sup>
kinO2anox	Half-saturation O2 inhib anoxic min	5	5	mmol m-3	L <sup>5</sup>
ksO2nitri	Half-saturation O2 in nitrification	100	100	mmol m-3	L <sup>5</sup>
ksO2oduox	Half-saturation O2 in oxidation of ODU	100	100	mmol m-3	L <sup>5</sup>
rODUox	Maximum rate oxidation of ODU	20	20	day <sup>-1</sup>	L <sup>5</sup>
rnit	Maximum nitrification rate	20	20	day <sup>-1</sup>	L <sup>5</sup>
NH3Ads	Adsorption coefficient ammonium	1.3	1.3		L <sup>5</sup>
roxidNO3	Maximum oxidation of ODU by NO3	200	200	day <sup>-1</sup>	L <sup>5</sup>
ksNO3ODUox	Half-saturation NO3 in Fe oxydation	200	200	mmol m-3	L <sup>5</sup>
kinO2ODUox	Half-saturation O2 in Fe oxydation	1	1	mmol m-3	L <sup>5</sup>

1211  
1212 Table 1. Parameters used in the final simulation of the early diagenesis part of the 4GFOR model. The source of  
1213 the parameter values is indicated as follows: C = constrained with the model using the measured data; I =  
1214 independently determined from field data; L = based on literature values, retrieved from: <sup>1</sup>Anschutz and  
1215 Chaillou (2009); <sup>2</sup>Durrieu de Madron et al. (1999); <sup>3</sup>Mouret et al. (2010); <sup>4</sup>Ogawa et al. (1973) ; <sup>5</sup>Soetaert et al.  
1216 (1996) ; <sup>6</sup>Schmidt et al. (2009).

1217 .  
1218 Compared to Mouret et al. (2010), the fractions of inert C<sub>org</sub> (0.153 and 0.26) were not changed. Of  
1219 the 0.2 and 0.215 parts (stations A and B, respectively) attributed to the newly created category  
1220 Corg<sub>int</sub>, compared to the observations of Mouret et al. (2010), the large majority (87.5 and 91.2% for  
1221 stations A and B) was taken from the labile C<sub>org</sub>, and the remaining part from the slowly decaying C<sub>org</sub>.  
1222 The presence of the four foraminiferal species was constrained with the boundary conditions listed in  
1223 Table 2, which determined whether they were present or not. In our first attempts, using the data of  
1224 station A, for deep infauna, we used a threshold value for nitrate of 2.5 μmol l<sup>-1</sup>. It turned out that at  
1225 station B, where the nitrate concentration diminishes rapidly with greater depth in the sediment, this

1226 threshold truncated the downward distribution of deep infauna. In order to better simulate our field  
1227 observations, we subsequently decreased the nitrate threshold for deep infauna to 0.05  $\mu\text{mol l}^{-1}$ .

1228

1229

	Oxygen	Nitrate
Shallow infauna A	>2.5 $\mu\text{mol l}^{-1}$	No nitrate limitation
Shallow infauna B	>2.5 $\mu\text{mol l}^{-1}$	No nitrate limitation
Intermediate infauna	No oxygen limitation	>2.5 $\mu\text{mol l}^{-1}$
Deep infauna	No oxygen limitation	>0.05 $\mu\text{mol l}^{-1}$

1230

1231

1232

1233

1234 Table 2. Threshold values of oxygen and nitrate concentrations for the four theoretical species of benthic  
1235 foraminifera.

1236 Finally, foraminiferal biomass was tuned to the observational data by changing the fractions of the  
1237 different types of  $C_{\text{org}}$  attributed to the four theoretical species of foraminifera, as shown in Table 3.

Station A – 1000 m	$C_{\text{orgfast}}$	$C_{\text{orgint}}$	$C_{\text{orgslow}}$
Shallow infauna A	0.0006	0.0006	0
Shallow infauna B	0.0003	0.0012	0
Intermediate infauna	0.0002	0.0004	0.00001
Deep infauna	0.0001	0.0001	0.00015

1238

Station B – 550 m	$C_{\text{orgfast}}$	$C_{\text{orgint}}$	$C_{\text{orgslow}}$
Shallow infauna A	0.0006	0.0006	0
Shallow infauna B	0.0003	0.0012	0
Intermediate infauna	0.004	0.00033	0.00001
Deep infauna	0.0001	0.00001	0.00011

1239

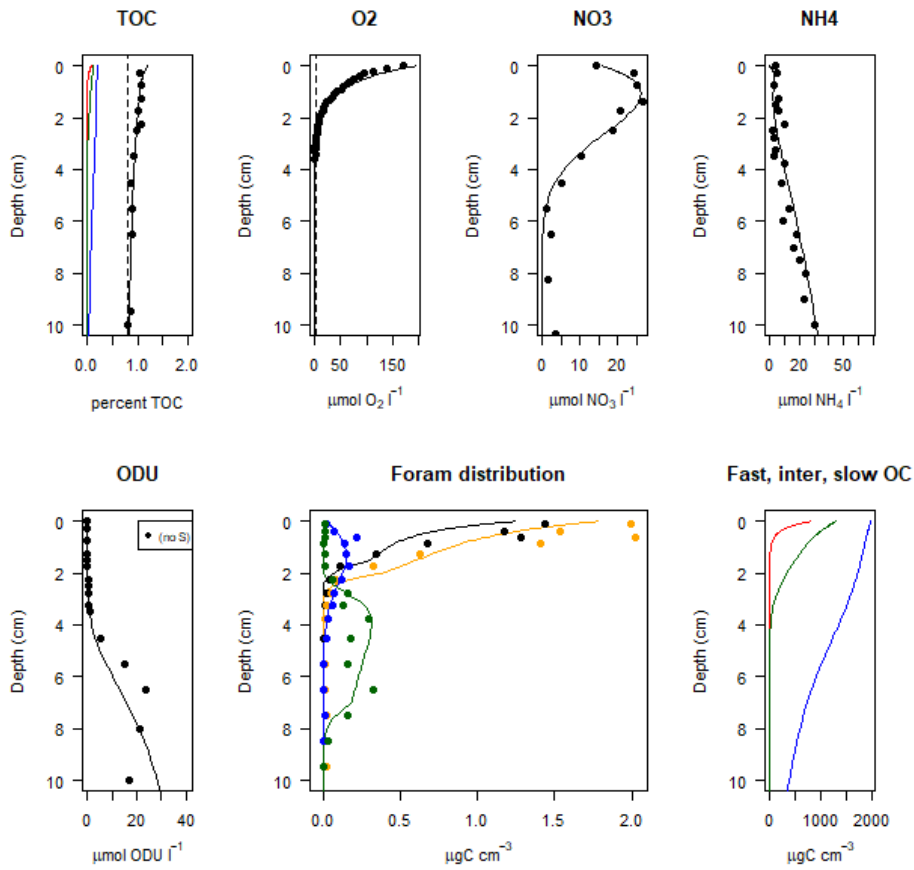
1240 Table 3. Fractions of the three types of reactive organic carbon attributed to each of the 4 theoretical species of  
1241 foraminifera, at stations A and B.

1242 The competitiveness of intermediate infauna/deep infauna with respect to highly and intermediately  
1243 reactive  $C_{\text{org}}$  further depends on oxygenation: it is low/very low under oxic conditions, and high/very  
1244 high under hypoxic/anoxic conditions.

1245 The final results of the tuning procedure of the 4GFOR model are shown in Fig. 5 and 6. As noted  
1246 earlier, the fit between the observed and modelled profiles of early diagenetic parameters is very  
1247 satisfactory. The two shallow infaunal species (A and B) are well separated in the top 1-2 cm of the  
1248 sediment, suggesting that our decision to differentiate them by their ability to cope with low quality  
1249  $C_{\text{org}}$  may be realistic. The profiles of intermediate and deep infaunal taxa correspond well with the  
1250 observed data, although in detail, the modelled distribution is slightly off for some levels.

1251

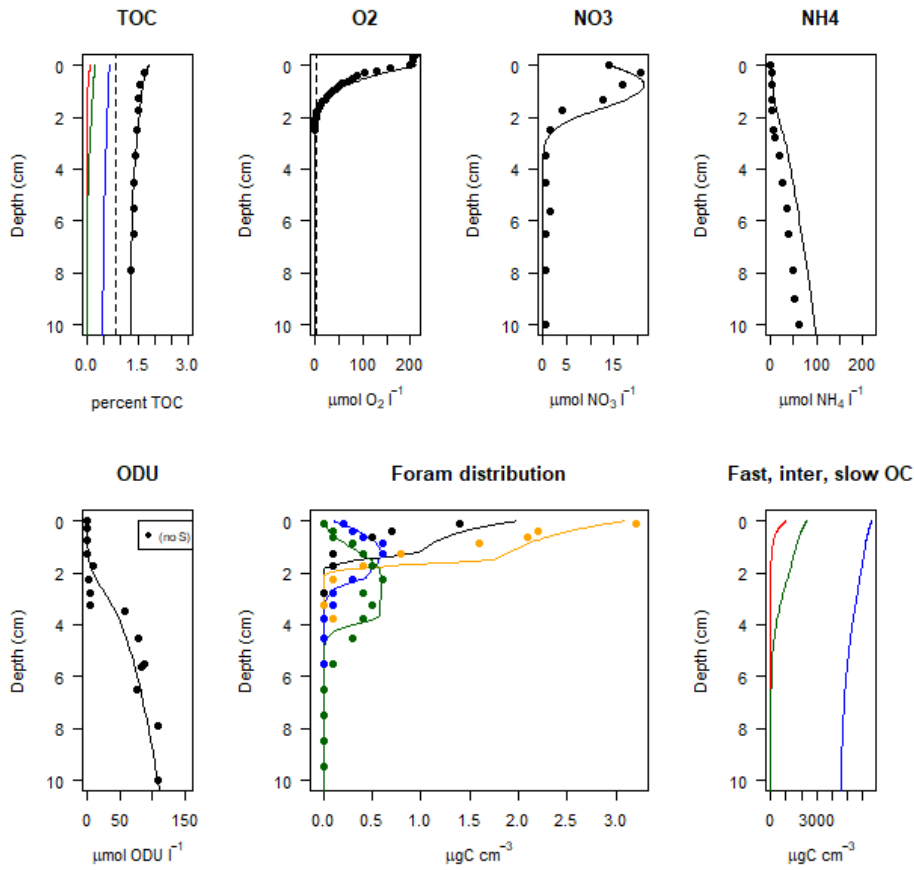
1252



1253

1254 Fig. 5. Final results for station A (1000 m depth) of the 4GFOR model with four types of organic matter (red:  
 1255 fast degrading, green: intermediate, blue: slow, and black: total TOC). Foraminiferal species distribution is  
 1256 represented as: Shallow Infauna A = black, Shallow Infauna B = orange, Intermediate Infauna = blue, Deep  
 1257 Infauna = green. All dots are averaged observed data, lines are model output.

1258



1259

1260 Fig. 6. Final results for station B (550 m depth) of the 4GFOR model with four types of organic matter (red: fast  
 1261 degrading, green: intermediate, blue: slow, and black: total TOC). Foraminiferal species distribution is  
 1262 represented as: Shallow Infauna A = black, Shallow Infauna B = orange, Intermediate Infauna = blue, Deep  
 1263 Infauna = green. All dots are averaged observed data, lines are model output.

1264

## 1265 9. Discussion

### 1266 9.1. Definition of organic matter

1267 The organic matter flux to the seafloor is composed of a large variety of particules, such as living  
 1268 microbial cells and secondary producers, detrital material, fecal pellets, other aggregates, and  
 1269 continental organic matter, as well as dissolved organic carbon (Middelburg, 1998). Consequently,  
 1270 particulate organic matter has a wide range of components, such as inert carbon, lipids, amino acids,  
 1271 vitamins and carbohydrates. These components have very different reactivities (Arndt et al., 2013). In  
 1272 models this range of organic matter can be represented in different ways, by two (2G), three (3G) or  
 1273 four (4G) groups with different reactivity, or, in the most sophisticated models, by a continuous  
 1274 range of organic matter quality. In the first version of our model, we used a 3G approach, with inert,

1275 reactive and less reactive C<sub>org</sub> types, whereas in the last (4G) version we added an intermediate  
1276 category, which allowed us to obtain much better simulations of the observational data.  
1277

## 1278 9.2. Characteristics of foraminiferal species

1279 While developing the 4GFOR model, the characteristics of our theoretical foraminiferal species have  
1280 progressively evolved, to become more complex. In our first runs, we attributed only fast degrading  
1281 C<sub>org</sub> to the shallow infaunal species. It turned out that because of the rapid decrease of C<sub>org-fast</sub> with  
1282 depth, compared to observational data, our model species did not penetrate deep enough into the  
1283 sediment. This example emphasizes the great importance of theoretical models: apparently the basic  
1284 hypothesis (= shallow infaunal taxa feed exclusively on C<sub>org-fast</sub>) was wrong, and consequently, the  
1285 model was incapable of simulating the observed data.

1286 We solved this problem by separating the group of shallow infaunal taxa into two species, SIA and  
1287 SIB, with SIB being much more tolerant to lower quality C<sub>org</sub> than SIA. The existence of two shallow  
1288 infaunal groups with different dominant test forms (SIA = trochospiral, planispiral; SIB = biserial,  
1289 triserial) is in accordance with abundant microhabitat observations in natural ecosystems and is  
1290 corroborated by the interspecific differences in the δ<sup>13</sup>C of their shells (e.g., McCorkle et al., 1990;  
1291 Rathburn et al., 1996; Fontanier et al., 2006b). By giving them access to different proportions of fast  
1292 degrading and intermediate C<sub>org</sub>, we could obtain a nearly perfect fit with the observed data.

1293 In our first trials, we used only a single deeper infaunal taxon, and we forced this species to remain at  
1294 depth in the sediment by limiting it to oxygen concentrations below 2.5 μmol l<sup>-1</sup>. In the later versions,  
1295 we separated this group into intermediate and deep infaunal taxa, in accordance with the large  
1296 volume of natural observations. Both groups were initially defined in such a way that they can only  
1297 occur when nitrate concentration is above 2.5 μmol l<sup>-1</sup>. In order to obtain a deeper penetration of  
1298 deep infauna at station B, we had to lower this threshold to 0.05 μmol l<sup>-1</sup> for this group. We further  
1299 differentiated intermediate and deep infauna by making DI more tolerant to low quality C<sub>org</sub> than II.  
1300 To avoid that these species invade the superficial sediment layers, where large amounts of highly  
1301 reactive C<sub>org</sub> are present, we added a competitive element, by attributing less C<sub>org-fast</sub> and C<sub>org-int</sub> to  
1302 these taxa when oxygen rises above 2.5 μmol l<sup>-1</sup>, with an exponential decrease towards higher  
1303 oxygen levels. With these characteristics, the overall distribution of II and DI is very close to the  
1304 observed patterns. This suggests that the way we defined these taxa may be correct, and that their  
1305 absence in the superficial sediment layers may indeed be the consequence of a strongly diminished  
1306 competitiveness in well oxygenated environments. In more general terms, this suggests that  
1307 interspecific competition for food particles may be an important controlling parameter.

1308 Finally, when tuning the model for two stations with very different characteristics, we managed to  
1309 obtain a good fit for the early diagenesis parameters while using the same reaction constants at both  
1310 stations. This underlines the robustness of this part of the model. In order to obtain good fits for the  
1311 foraminiferal data at both stations, we had to attribute slightly different proportions of the different  
1312 organic matter types to the four theoretical species (Table 3). This suggests that the foraminiferal  
1313 contribution to organic matter remineralisation may change as a function of the environmental  
1314 conditions.

## 1315 9.3. Perspectives

1316 Here, we present the newly developed 4GFOR model, and our tuning with the data of two sampling  
1317 stations at 1000 and 550 m depth in the Bay of Biscay, on the basis of averaged data of 10 successive  
1318 sampling campaigns. In view of the obtained simulations, which are very close, both for geochemical

1319 as for foraminiferal species, it appears that the complexity of the model is enough to correctly  
1320 represent the four main groups of foraminifera. The next step will be to test the model in different  
1321 environmental settings. We will accomplish this by modelling 1) the 10 successive sample times  
1322 individually, 2) the 9 other stations of the Bay of Biscay transect, between 140 and 4800 m depth,  
1323 with a wide range of environmental characteristics, 3) sampling stations from other ocean basins  
1324 (Indian Ocean, Cape Blanc upwelling) from which we have comparable data sets. These modelling  
1325 exercises will very probably lead to adjustments of the model, and the way the foraminiferal species  
1326 are defined. This will oblige us to consider slightly different ecological strategies for the four species,  
1327 and thereby, to test many hypotheses we still have regarding their life strategies.

1328 Once the robustness of the 4GFOR model has been fully demonstrated, the next step will be to  
1329 develop a formal inversion of the model, so that the main parameters controlling the foraminiferal  
1330 faunas, the quantity and quality of the organic flux to the sea floor and the vertical succession of  
1331 redox species, can be reconstructed on the basis of the composition of fossil faunas in sediment  
1332 cores and outcrops.

## 1333 10. Conclusion

1334 The 4GFor model is a combination of an early diagenetic model, based on the OMEXDIA model of  
1335 Soetaert et al. (1996), and a transformation model, which transforms proportions of organic matter  
1336 types with different reaction rates into foraminiferal biomass. Foraminiferal communities are  
1337 simulated with four theoretical deep water species. Their different tolerance levels with respect to  
1338 oxygen and nitrate concentrations decide at what depths they can occur, whereas their density is  
1339 mainly controlled by organic matter quality.

1340 .

1341 The model has been tuned to a large geochemical and foraminiferal database of two stations, at  
1342 1000 and 550 depth in the Bay of Biscay. The outcome shows that the early diagenesis part of the  
1343 model correctly reproduces the vertical distribution of redox species in the top 10 cm of the  
1344 sediment. By attributing various proportions of the different types of organic matter to the four  
1345 foraminiferal species, the model adequately reproduces the vertical succession of shallow,  
1346 intermediate and deep infaunal species.

1347 The model further separates shallow infaunal taxa into two groups. Group SIA, which is found close  
1348 to the sediment-water interface, corresponds to trochospiral (e.g., *Cibicidoides*, *Gyroidina*,  
1349 *Hoeglundina*) and planispiral species (e.g., *Cassidulina*). This group is critically sensitive to food  
1350 quality. Group SIB, which is found slightly deeper in the sediment, corresponds to triserial (e.g.,  
1351 *Bulimina*, *Uvigerina*) and biserial (e.g., *Bolivina*) taxa, which are less restrictive with respect to food  
1352 quality. The observed distribution of these groups at the two stations in the Bay of Biscay is  
1353 reproduced by the model. Also the depth in the sediment of intermediate (e.g., *Melonis barleeanus*)  
1354 and deep infaunal (e.g., *Globobulimina* spp.) species is very well simulated.

1355 The tuning of the model indicates that shallow infaunal taxa (neither SIA nor SIB) do not feed  
1356 exclusively on the most labile  $C_{org}$  component. Their vertical distribution can only be simulated by  
1357 giving them access to slightly less reactive  $C_{org}$ .

1358 One of the problems encountered during the tuning phase was to keep intermediate and deep  
1359 infaunal taxa restricted to deeper layers. Because of the presence of large quantities of high quality  
1360  $C_{org}$  close to the sediment surface, this layer is also attractive for those species. To solve this problem,

1361 we diminished their competitive ability exponentially towards higher oxygen levels. This solution  
1362 appears to be realistic, but should be tested in experimental conditions.

1363 As is shown by these first examples, the 4GFOR model can be a powerful tool to help understand  
1364 foraminiferal ecology. In the future, we intend to construct a formal inversion of the model, which  
1365 will make it possible to produce quantitative estimates of the main controlling faunal parameters  
1366 (quantity and quality of the organic flux, oxygen and nitrate concentration) on the basis of the  
1367 composition of fossil foraminiferal assemblages.

#### 1368 **11. Acknowledgements**

1369 The authors are grateful to Karline Soetaert for her help with the addition of the ferrous iron  
1370 nitrification reactions to the early diagenesis model.

**Commenté [f2]:** Explain how migration is taken into account

1371 **12. References**

- 1372 Alve, E., Bernhard, J.M., 1995. Vertical migratory response of benthic foraminifera to controlled  
1373 oxygen concentrations in an experimental mesocosm. *Marine Ecology Progress Series*, 116, 137-151.
- 1374 Anschutz, P., Chaillou, G., 2009. Deposition and fate of reactive Fe, Mn, P and C in suspended  
1375 particulate matter in the Bay of Biscay. *Continental Shelf Research* 29, 1038-1043.
- 1376 Anschutz, P., Dedieu, K., Desmazes, F., Chaillou, G., 2005. Speciation, oxidation state, and reactivity  
1377 of particulate manganese in marine sediments. *Chem. Geol.*, 218, 265–279.
- 1378 Anschutz, P., Hyacinthe, C., Carbonel, P., Jouanneau, J.M., Jorissen, F.J., 1999. The distribution of  
1379 inorganic phosphorus in modern sediments of the Bay of Biscay. *C.R. Acad. Sci. Paris*, 328, 765-771.
- 1380 Arndt, S., Jørgensen, B.B., LaRowe, D.E., Middelburg, J.J., Pancost, R.D., Regnier, P., 2013.  
1381 Quantifying the degradation of organic matter in marine sediments: A review and synthesis. *Earth-*  
1382 *Science Reviews*, 123, 53–86.
- 1383 Bernhard, J.M., 1986. Characteristic assemblages and morphologies of benthic foraminifera from  
1384 anoxic, organic-rich deposits: Jurassic through Holocene.
- 1385 Bernhard, J.M., 1993. Experimental and field evidence of Antarctic foraminiferal tolerance to anoxia  
1386 and hydrogen sulfide. *Marine Micropaleontology*, 20, 203-213. *Journal of Foraminiferal research*, 16,  
1387 207-215.
- 1388 Bernhard, J.M., Alve, E., 1996. Survival, ATP pool, and ultrastructural characterization of benthic  
1389 foraminifera from Drammensfjord (Norway): response to anoxia. *Marine Micropaleontology*, 28, 5-  
1390 17.
- 1391 Bernhard, J.M., Bowser, S.S., 1999. Benthic foraminifera of dysoxic sediments: chloroplast  
1392 sequestration and functional morphology. *Earth-Science Reviews*, 46, 149–165.
- 1393 Bernhard, J. M., Casciotti, K. L., McIlvin, M. R., Beaudoin, D.J., Visscher, P. T., Edgcomb, V. P.,  
1394 2012. Potential importance of physiologically diverse benthic foraminifera in sedimentary nitrate  
1395 storage and respiration. *J. Geophys. Res.*, 117, G03002, doi:10.1029/2012JG001949, 2012.
- 1396 Canfield, D.E., Jørgensen, B.B., Fossing, H., Glud, R., Gundersen, J., Ramsing, N.B., Thamdrup, B.,  
1397 Hansen, J.W., Nielsen, L.P., Hall, P.O.J., 1993. Pathways of organic carbon oxidation in three  
1398 continental margin sediments. *Mar. Geol.* 113, 27-40.
- 1399 Carney, R. S., 2005. Zonation of deep biota on continental margins. *Oceanography and Marine*  
1400 *Biology. Annual Review*, 43, 211–278.
- 1401 Chaillou, G., Anschutz, P., Lavaux, G., Blanc, G., 2006. Rare earth elements in the modern sediments  
1402 of the Bay of Biscay (France). *Mar. Chem.*, 100, 39–52.
- 1403 Chaillou, G., Anschutz, P., Lavaux, G., Schäfer, J., Blanc, G., 2002. The distribution of Mo, U, and Cd  
1404 in relation to major redox species in muddy sediments of the Bay of Biscay. *Mar. Chem.*, 80, 41–59.
- 1405 Chaillou, G., Schäfer, J., Anschutz, P., Lavaux, G., Blanc, G., 2003. The behaviour of arsenic in  
1406 muddy sediments of the Bay of Biscay (France). *Geochim. Cosmochim. Acta*, 67, 2993–3003.
- 1407 Charbonnier C., Mouret A., Howa H., Schmidt S., Gillet H., Anschutz P. 2019. Quantification of  
1408 diagenetic transformation of continental margin sediments at the Holocene time scale. *Continental*  
1409 *Shelf Research*, 180, 63-74.
- 1410 Corliss, B.H., 1985. Microhabitats of benthic foraminifera within deep-sea sediments: *Nature*, v. 314,  
1411 p. 435-438.
- 1412 Corliss, B.H., Chen, C., 1988, Morphotype patterns of Norwegian Sea deep-sea benthic foraminifera  
1413 and ecological implications: *Geology*, v. 16, p. 716-719.
- 1414 Corliss, B.H., Emerson, S., 1990. Distribution of Rose Bengal stained deep-sea benthic foraminifera  
1415 from the Nova Scotian continental margin and Gulf of Maine. *Deep-Sea Research*, 37, 381-400.
- 1416 Fontanier, C., Jorissen, F.J., Licari, L., Alexandre, A., Anschutz, P., Carbonel, P., 2002. Live benthic  
1417 foraminiferal faunas from the Bay of Biscay; faunal density, composition and microhabitats. *Deep-Sea*  
1418 *Research*, I, 49, 751-785.

1419 Fontanier, C., Jorissen, F.J., Chaillou, G., David, C., Anschutz, P., Lafon, V., 2003. Seasonal and  
1420 interannual variability of benthic foraminiferal faunas at 550 m depth in the Bay of Biscay. *Deep-Sea*  
1421 *Research*, I, 50, 457-494.

1422 Fontanier C., Jorissen F.J., Chaillou G., Anschutz P., Grémare A., Griveaud C., 2005. Live  
1423 foraminiferal faunas from a 2800 m deep lower canyon station from the Bay of Biscay: Faunal  
1424 response to focusing of refractory organic matter. *Deep-Sea Research*, I, 52, 1189-1227.

1425 Fontanier, C., Jorissen, F.J., Anschutz, P., Chaillou, G., 2006a. Seasonal variability of benthic  
1426 foraminiferal faunas at 1000 m depth in the Bay of Biscay. *Journal of Foraminiferal research*, 36, 61-  
1427 76.

1428 Fontanier, C., Mackensen, A., Jorissen, F.J., Anschutz, P., Licari, L., Griveaud, C. 2006b. Stable  
1429 oxygen and carbon isotopes of live benthic foraminifera from the Bay of Biscay: Microhabitat impact  
1430 and seasonal variability. *Marine Micropaleontology*, 58, 159-183.

1431 Froelich, P.N., Klinkhammer, G.P., Bender, M.L., Luedke, N.A., Heath, G.R., Cullen, D., Dauphin, P.,  
1432 Hammond, D., Hartman, B., Maynard, V., 1979. Early oxidation of organic matter in pelagic  
1433 sediments of the Eastern Equatorial Atlantic: suboxic diagenesis. *Geochim. Cosmochim. Acta* 43,  
1434 1075-1090.

1435 Geslin, E., Risgaard-Petersen, N., Lombard, F., Metzger, E., Langlet, D., Jorissen, F.J., 2011. Oxygen  
1436 respiration rates of benthic foraminifera as measured with oxygen microsensors. *Journal of*  
1437 *Experimental Marine Biology and Ecology*, 396, 108-114.

1438 Gooday, A.J., 1986. Meiofaunal foraminifera from the bathyal Porcupine Seabight (northeast  
1439 Atlantic): Size structure, standing stock, taxonomic composition, species diversity and vertical  
1440 distribution in the sediment. *Deep-Sea Research*, 33, 1345-73.

1441 Henrichs, S.M., 1992. Early diagenesis of organic matter in marine sediments: progress and  
1442 perplexity. *Marine Chemistry*, 39, 119-149.

1443 Herguera, J. C., Berger, W., 1991. Paleoproductivity from benthonic foraminifera abundance: Glacial  
1444 to postglacial change in the west-equatorial Pacific. *Geology*, 19, 1173-1176.

1445 Høglund, S., Revsbech, N.P., Cedhagen, T., Nielsen, L.P., Gallardo, V.A., 2008. Denitrification,  
1446 nitrate turnover, and aerobic respiration by benthic foraminifera in the oxygen minimum zone off  
1447 Chile. *J. Exp. Mar. Biol. Ecol.*, 359, 85-91.

1448 Hyacinthe, C., Anschutz, P., Carbonel, C., Jouanneau, J.M., Jorissen, F.J. 2001. Early diagenetic  
1449 processes in muddy sediments of the Bay of Biscay. *Marine Geology*, 177, 111-128.

1450 Jauffrais, T., Jesus, B., Metzger, E., Mouget, J.L., Jorissen, F., Geslin, E., 2016. Effect of light on  
1451 photosynthetic efficiency of sequestered chloroplasts in intertidal benthic foraminifera (*Haynesina*  
1452 *germanica* and *Ammonia tepida*). *Biogeosciences*, 13, 2715-2726.

1453 Jorissen, F.J., 1999a. Benthic foraminiferal microhabitats below the sediment-water interface. In: Sen  
1454 Gupta, B. (ed.): *Ecology of recent foraminifera*, Kluwer Academic Publishers, chapter 10, p. 161-179.

1455 Jorissen, F.J., 1999b. Benthic foraminiferal successions across Late Quaternary Mediterranean  
1456 Sapropels. *Marine Micropaleontology*, 153, 91-101.

1457 Jorissen, F.J., De Stigter, H.C., Widmark, J.G.V. (1995) A conceptual model explaining benthic  
1458 foraminiferal microhabitats. *Marine Micropaleontology*, 26, 3-15.

1459 Jorissen, F.J., Fontanier, C., Thomas, E., 2007. Paleoceanographical proxies based on deep-sea benthic  
1460 foraminiferal assemblage characteristics. In: Hillaire-Marcel, C., and De Vernal, A. (eds.): *Proxies in*  
1461 *Late Cenozoic Paleoceanography*. Elsevier Publishers. *Developments in Marine Geology*, 1, 263-325.

1462 Jorissen, F.J., Wittling, I., Peypouquet, J.P., Rabouille, C., Relexans, J.C., 1998. Live benthic  
1463 foraminiferal faunas off Cap Blanc, NW Africa; community structure and microhabitats: *Deep-Sea*  
1464 *Research* I, 45, p. 2157-2188.

1465 Kappler, A., Bryce, C., Mansor, M., Byrne, J.M., Swanner, E.D., 2021. An evolving view on  
1466 biogeochemical cycling of iron. *Nature reviews microbiology*, 19, 360-374.

1467 Koho, K.A., De Nooijer, L.J., Reichart, G.J., 2015. Combining benthic foraminiferal ecology and shell  
1468 Mn/Ca to deconvolve past bottom water oxygenation and paleoproductivity. *Geochim. Cosmochim.*  
1469 *Acta*, 165, 294-306.

1470 Langezaal, A.M., Jorissen, F.J., Braun, B., Chaillou, G., Fontanier, C., Anschutz, P., Van der Zwaan,  
1471 G.J., 2006. The influence of seasonal processes on geochemical profiles and foraminiferal assemblages  
1472 on the outer shelf of the Bay of Biscay. *Continental Shelf research*, 26, 1730-1755.

1473 Langlet, D., Baa, C., Geslin, E., Metzger, E., Zuschin, M., Riedel, B., Risgaard-Petersen, N.,  
1474 Stachowitsch, M., Jorissen, F.J., 2014. Foraminiferal species responses to in situ, experimentally  
1475 induced anoxia in the Adriatic Sea. *Biogeosciences*, 11, 1775-1797.

1476 Lee, J.J., Anderson, O.R., 1991. Symbiosis in Foraminifera. In: Lee, J.J., Anderson, O.R. (Eds.),  
1477 *Biology of Foraminifera*. Academic Press, London, pp. 157-220.

1478 Leutenegger, S., 1984. Symbiosis in benthic foraminifera: specificity and host adaptations. *J.*  
1479 *Foraminiferal Res.*, 14, 16-35.

1480 Loubere, P., Gary, A., Lagoe, M., 1993. Benthic foraminiferal microhabitats and the generation of a  
1481 fossil assemblage: Theory and preliminary data. *Marine Micropaleontology*, 20, 165-181.

1482 Mackensen, A., Douglas, R.G., 1989. Down-core distribution of live and dead deep-water benthic  
1483 foraminifera in box cores from the Weddell Sea and the California continental borderland. *Deep-Sea*  
1484 *Research*, 36, 879-900.

1485 McCorkle, D.C., Keigwin, L.D., Corliss, B.H., Emerson, S.R., 1990. The influence of microhabitats  
1486 on the carbon isotopic composition of deep-sea benthic foraminifera. *Paleoceanography*, 5, 161-85.

1487 Middelburg J.J., 2018. Reviews and syntheses: to the bottom of carbon processing at the seafloor  
1488 *Biogeosciences*, 15, 413-427.

1489 Middelburg, J.J., 2019. *Marine Carbon Biogeochemistry. A Primer for Earth System Scientists.*  
1490 SpringerBriefs in Earth System Sciences. 188pp.

1491 Mojtahid, M., Griveaud, C., Fontanier, C., Anschutz, P., Jorissen, F.J., 2010. Live benthic  
1492 foraminiferal faunas along a bathymetrical transect (140-4800 m) in the Bay of Biscay (NE Atlantic).  
1493 *Revue de Micropaléontologie*, 53, 139-162.

1494 Moodley, L., Schaub, B.E.M., Van der Zwaan, G.J., Herman, P.M.J., 1998. Tolerance of benthic  
1495 foraminifera (Protista: Sarcodina) to hydrogen sulphide. *Marine Ecology Progress Series*, 169, 77-86.  
1496

1497 Mouret A., Anschutz P., Chaillou G., Hyacinthe C., Deborde J., Lecroart, P., Jorissen F.J., Deflandre  
1498 B., Schmidt S., Jouanneau J.M., 2009. Benthic geochemistry of manganese in the Bay of Biscay. *Geo-*  
1499 *Marine Letters*, 29, 133-149.

1500 Mouret, A., Anschutz, P., Deflandre, B., Chaillou, G., Hyacinthe, C., Deborde, J., Etcheber, H.,  
1501 Jouanneau, J.M., Grémare, A., Lecroart, P., 2010. Oxygen and organic carbon fluxes in sediments of  
1502 the Bay of Biscay. *Deep-Sea Research I*, 528-540.

1503 Mouret A., Anschutz P., Deflandre B., Deborde J., Canton M., Poirier D., Grémare A., Howa H.,  
1504 2016. Spatial heterogeneity of benthic biogeochemistry in two contrasted marine environments  
1505 (Arcachon bay and Bay of Biscay, SW France). *Estuarine, Coastal and Shelf Science* 179, 51-65.

1506 Nomaki, H., Yamaoka, A., Shirayama, Y., Kitazato, H., 2007. Deep-sea benthic foraminiferal  
1507 respiration rates measured under laboratory conditions. *J. Foraminif. Res.*, 37, 281-286.

1508 Ogawa, N., Tauzin, P., 1973. Contribution à l'étude hydrologique et géochimique du Golfe de Cap-  
1509 Breton. *Bulletin de l'Institut Géologique du Bassin d'Aquitaine, Bordeaux*, 14, 19-46.

1510 Pina-Ochoa, E., Hogslund, S., Geslin, E., Cedhagen T., Revsbech, N.P., Nielsen, L.P., Schweizer, M.,  
1511 Jorissen, F.J., Risgaard, S., Risgaard-Petersen, N., 2010. Widespread occurrence of nitrate storage and  
1512 denitrification among Foraminifera and Gromiida. *PNAS* doi:10.1073/pnas.0908440107.

1513 Rathburn, A.E., Corliss, B.H., 1994. The ecology of living (stained) deep-sea benthic foraminifera  
1514 from the Sulu Sea: *Paleoceanography*, v. 9, p. 87-150.

1515 Rathburn, A.E., Corliss, B.H., Tappa, K.D., Lohmann, K.C., 1996. Comparison of the ecology and  
1516 stable isotopic compositions of living (stained) benthic foraminifera from the Sulu and South  
1517 China Seas. *Deep-Sea Research* 43, 1617- 1646.

1518 R Core Team, 2020. R: A Language and Environment for Statistical Computing. R Foundation for  
1519 Statistical Computing, Vienna.

1520 Richirt, J., Riedel, B., Mouret, A., Schweizer, M., Langlet, D., Seitaj, D., Meysman, F.J.R., Slomp,  
1521 C.P., Jorissen, F.J., 2020. Foraminiferal community response to seasonal anoxia in Lake Grevelingen  
1522 (the Netherlands). *Biogeosciences*, 17, 1415–1435, 2020.

1523 Risgaard-Petersen N, Langezaal, A.M., Ingvaridsen, S., Schmid, M.C., Jetten, M.S.M., Op den Camp,  
1524 H.J.M., Derksen, J.W.M., Pina-Ochoa, E., Eriksson, S.P., Nielsen, L.P., Revsbech, N.P., Cedhagen,  
1525 T., Van der Zwaan, G.J., 2006. Evidence for complete denitrification in a benthic foraminifer. *Nature*,  
1526 443, 93–96. Ross, B.J., Hallock, P., 2016. Dormancy in the foraminifera: a review. *J. Foram. Res.*, 46,  
1527 358–368.

1528 Schmidt, S., Howa, H., Mouret, A., Lombard, F., Anschutz, P., Labeyrie, L., 2009. Particle fluxes and  
1529 recent sediment accumulation on the Aquitanian margin of Bay of Biscay. *Continental Shelf Research*,  
1530 29, 1044–1052.

1531 Shirayama, Y., 1984. Vertical distribution of meiobenthos in the sediment profile in bathyal, abyssal  
1532 and hadal deep sea systems of the western Pacific. *Oceanologica Acta*, 7, 123–29.

1533 Soetaert, K., Meysman, F., 2012. Reactive transport in aquatic ecosystems: Rapid model prototyping  
1534 in the open source software R *Environmental Modelling & Software*, 32, 49–60.

1535 Soetaert K, Herman, P.M.J., Middelburg, J.J., 1996. A model of early diagenetic processes from the  
1536 shelf to abyssal depths. *Geochim. Cosmochim. Acta*, 60, 1019–1040.

1537 Soetaert K., Herman, P.M.J., 2009. A practical guide to ecological Modelling - using R as a simulation  
1538 platform. Springer, 377 pp.

1539 Straub, K.L., Benz, M., Schink, B., Widdel, F., 1996. Anaerobic, Nitrate-Dependent Microbial  
1540 Oxidation of Ferrous Iron. *Applied and Environmental Microbiology*, 62, 1458–1460. Van der Zwaan, G. J.,  
1541 Duijnste I. A. P., Den Dulk M., Ernst S. R., Jannink N. T., Kouwenhoven T. J., 1999. Benthic  
1542 foraminifers: proxies or problems? A review of paleocological concepts. *Earth Sci. Rev.* 46, 213–236.  
1543  
1544